



HAL
open science

Long-term safety and efficacy of lentiviral hematopoietic stem/progenitor cell gene therapy for Wiskott–Aldrich syndrome

A. Magnani, M. Semeraro, F. Adam, C. Booth, Loïc Dupré, E. Morris, A. Gabrion, C. Roudaut, D. Borgel, A. Toubert, et al.

► To cite this version:

A. Magnani, M. Semeraro, F. Adam, C. Booth, Loïc Dupré, et al.. Long-term safety and efficacy of lentiviral hematopoietic stem/progenitor cell gene therapy for Wiskott–Aldrich syndrome. *Nature Medicine*, 2022, 28 (1), pp.71-80. 10.1038/s41591-021-01641-x . hal-03776861

HAL Id: hal-03776861

<https://hal.science/hal-03776861>

Submitted on 13 Feb 2024

HAL is a multi-disciplinary open access archive for the deposit and dissemination of scientific research documents, whether they are published or not. The documents may come from teaching and research institutions in France or abroad, or from public or private research centers.

L'archive ouverte pluridisciplinaire **HAL**, est destinée au dépôt et à la diffusion de documents scientifiques de niveau recherche, publiés ou non, émanant des établissements d'enseignement et de recherche français ou étrangers, des laboratoires publics ou privés.



OPEN

Long-term safety and efficacy of lentiviral hematopoietic stem/progenitor cell gene therapy for Wiskott–Aldrich syndrome

A. Magnani^{1,2,31}, M. Semeraro^{3,31}, F. Adam⁴, C. Booth^{5,6}, L. Dupré^{7,8,9}, E. C. Morris^{10,11}, A. Gabrion^{1,2}, C. Roudaut^{1,2}, D. Borgel^{4,12}, A. Toubert^{13,14}, E. Clave¹³, C. Abdo^{15,16}, G. Gorochov^{17,18}, R. Petermann¹⁹, M. Guiot¹, M. Miyara^{17,18}, D. Moshous^{20,21}, E. Magrin^{1,2}, A. Denis²², F. Suarez^{21,23}, C. Lagresle²², A. M. Roche²⁴, J. Everett²⁴, A. Trinquand^{15,16}, M. Guisset⁷, J. Xu Bayford⁵, S. Hacein-Bey-Abina^{25,26}, A. Kauskot⁴, R. Elfeky⁵, C. Rivat⁵, S. Abbas²⁷, H. B. Gaspar⁵, E. Macintyre^{15,16}, C. Picard^{21,28}, F. D. Bushman²⁴, A. Galy^{27,29}, A. Fischer^{20,21,30,32}, E. Six^{22,32}, A. J. Thrasher^{5,6,32} and M. Cavazzana^{1,2,21,32}

Patients with Wiskott–Aldrich syndrome (WAS) lacking a human leukocyte antigen-matched donor may benefit from gene therapy through the provision of gene-corrected, autologous hematopoietic stem/progenitor cells. Here, we present comprehensive, long-term follow-up results (median follow-up, 7.6 years) (phase I/II trial no. [NCT02333760](#)) for eight patients with WAS having undergone phase I/II lentiviral vector-based gene therapy trials (nos. [NCT01347346](#) and [NCT01347242](#)), with a focus on thrombocytopenia and autoimmunity. Primary outcomes of the long-term study were to establish clinical and biological safety, efficacy and tolerability by evaluating the incidence and type of serious adverse events and clinical status and biological parameters including lentiviral genomic integration sites in different cell subpopulations from 3 years to 15 years after gene therapy. Secondary outcomes included monitoring the need for additional treatment and T cell repertoire diversity. An interim analysis shows that the study meets the primary outcome criteria tested given that the gene-corrected cells engrafted stably, and no serious treatment-associated adverse events occurred. Overall, severe infections and eczema resolved. Autoimmune disorders and bleeding episodes were significantly less frequent, despite only partial correction of the platelet compartment. The results suggest that lentiviral gene therapy provides sustained clinical benefits for patients with WAS.

Wiskott–Aldrich syndrome (WAS) is a complex X-linked disorder caused by loss-of-function mutations in the WAS gene encoding WAS protein (WASp), a key regulator of the actin cytoskeleton in hematopoietic cells¹. WASp deficiency causes characteristic microthrombocytopenia and lymphoid–myeloid dysfunction, the severity of which usually depends on the residual levels of WASp expression and function. WAS affects all the hematopoietic cellular compartments, which explains the broad range of associated clinical manifestations^{1–3}. The Zhu score⁴ is commonly used to stratify disease severity. The most severe phenotype is characterized by susceptibility to severe infection, bleeding, eczema, autoimmunity and a risk of malignancy^{3,6}. Without a curative treatment for WAS, most patients lacking functional WASp do not survive beyond their second or third decade of life⁷.

The most severe, early-onset, life-threatening form of WAS is characterized by profound, treatment-refractory thrombocytopenia⁶. At the other end of the WAS severity spectrum, X-linked thrombocytopenia (XLT) represents a milder disease entity. It is primarily characterized by microthrombocytopenia, although patients with XLT can also develop classical complications of WAS.

The first-line treatment for WAS is allogeneic hematopoietic stem cell transplantation (HSCT) with a human leukocyte antigen (HLA)-compatible donor. Although transplantation was initially associated with substantial mortality and morbidity rates, outcomes

have substantially improved^{8–11}. In the most recently described cohort of patients with WAS having undergone HSCT¹², the overall survival rate was 94% for those treated before the age of 5 years. The rate fell to 66% in those treated at an older age. The outcome after HSCT is influenced by the level of donor engraftment. Mixed donor chimerism after HSCT is associated with an increased risk of poor immune reconstitution and autoimmunity. In particular, donor myeloid engraftment below 50% is associated with persistent thrombocytopenia^{8,9,11,12}. In addition, between 10% and 20% of long-term survivors have active autoimmune complications, which are closely linked to the level of mixed chimerism (<70%)^{8,9}.

For patients lacking a suitable donor for HSCT, other treatment options have been developed. These include haplo-identical HSCT and gene therapy via the infusion of gene-corrected autologous hematopoietic stem cells (HSCs). Haplo-identical transplantation is an attractive option because a family member is almost always available as a donor for pediatric patients. Moreover, the high morbidity and mortality rates initially associated with this approach⁸ are now falling^{11–13}.

The gene therapy approach bypasses many of the remaining problems associated with haplo-identical HSCT, in particular the toxicity of a full conditioning regimen and the risk of graft-versus-host disease. A rationale for gene therapy has been provided by natural somatic reversion events reported in a number of patients with

A full list of affiliations appears at the end of the paper.

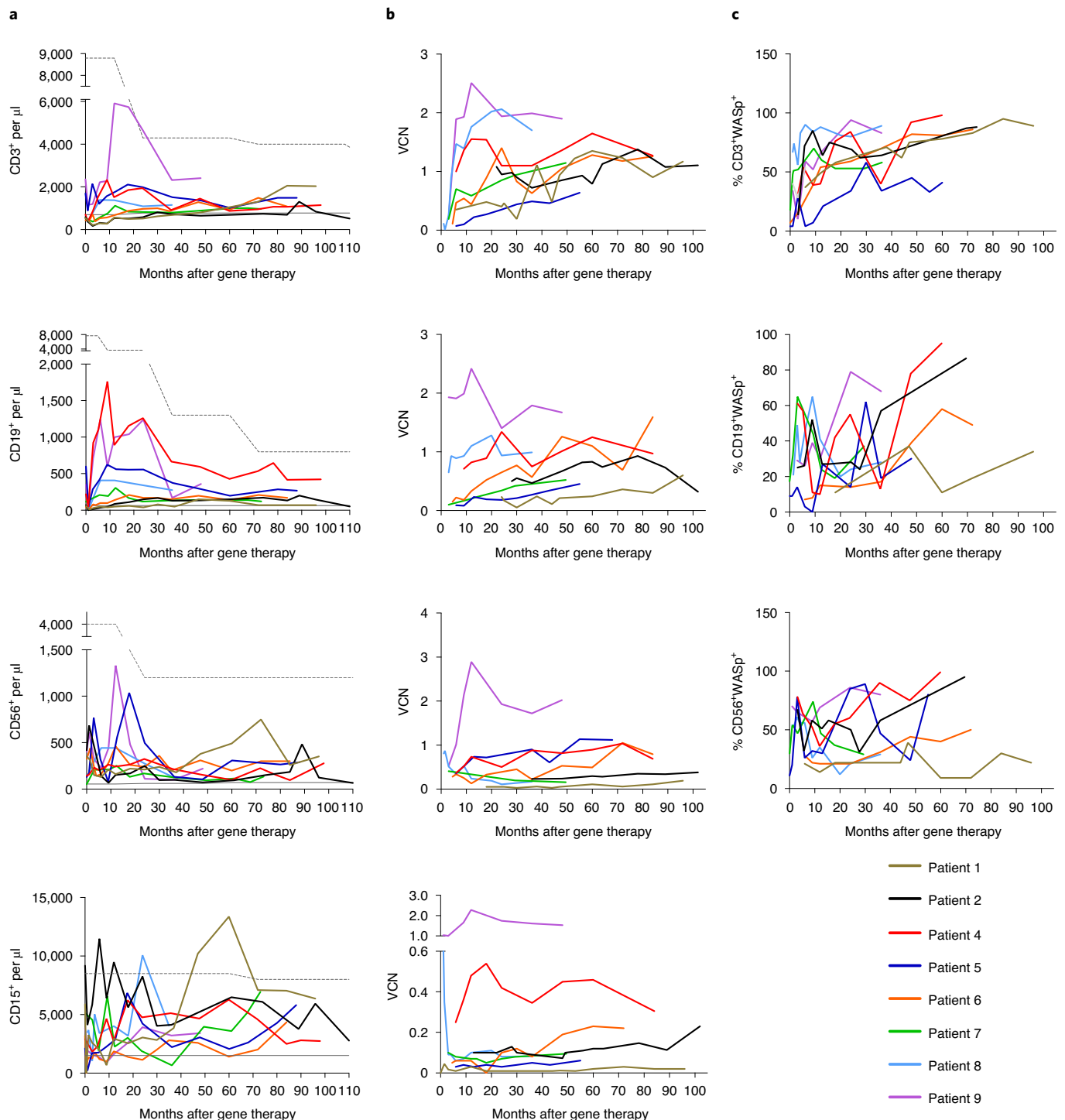


Fig. 1 | Immune reconstitution after gene therapy. **a**, Measurement of the total CD3⁺ T cell, CD19⁺ B cell, CD56⁺ natural killer (NK) cell and CD15⁺ neutrophil counts in blood at regular time points after gene therapy. Age-matched reference values are indicated by the gray lines (solid line, lower value; dashed line, upper value). **b**, Measurement of the VCN per cell at regular time points after gene therapy as a guide to the level of gene marking in CD3⁺ T cells, CD19⁺ B cells, CD56⁺ NK cells and CD15⁺ neutrophils (top to bottom). **c**, Change over time in the proportion of WASp-positive CD3⁺ T cells, CD19⁺ B cells and CD56⁺ NK cells after gene therapy.

WAS^{14–16}. In such cases, the accumulation of WASp-expressing lymphocytes constitutes direct evidence of the *in vivo* selective advantage of genetically competent cells. A previous trial using a gamma retroviral vector with a viral promoter provided evidence for the efficacy of gene therapy for WAS¹⁷. Unfortunately, this treatment was associated with serious adverse events related to vector-mediated

insertional mutagenesis in all of the patients¹⁸. To minimize mutagenic side effects, subsequent phase I/II clinical trials have been based on the use of a self-inactivating lentiviral vector expressing WASp under the control of a minimal endogenous promoter^{19–21}. These studies have confirmed the efficacy of gene therapy for WAS, and no major safety concerns were highlighted.

We have previously reported the results of 9- to 42-month follow-up of seven pediatric patients with severe WAS enrolled in non-randomized, open-label, phase I/II gene therapy clinical studies (nos. NCT01347346 and NCT01347242) (ref. ²⁰). Here, we report comprehensive, long-term follow-up efficacy and safety data (4–9 years after gene therapy; median, 7.6 years) for these and two additional patients (including a young adult patient) enrolled after the first report.

Results

Clinical presentation. We previously reported on non-randomized, open-label, phase I/II clinical studies (based on a lentiviral gene therapy vector) involving seven pediatric patients (referred to hereafter as patients 1–7) with severe WAS. The patients were treated at Necker-Enfants Malades Hospital (Paris, France) and at Great Ormond Street Hospital (London, UK)²⁰. One patient (patient 3) died 7 months after gene therapy from pre-existing complications of infection, as reported previously²⁰. Since the initial report, two additional patients treated at the Royal Free London Hospital and Great Ormond Street Hospital have been followed for at least 4 years after gene therapy and were included in the present study (patients 8 and 9). Patient 8 presented with severe cutaneous vasculitis, arthropathy, lymphoproliferation and chronic kidney disease requiring intensive immunosuppressive treatment and splenectomy before gene therapy²². Patient 9 had presented with gastrointestinal bleeding, severe eczema, recurrent infections, cytomegalovirus viremia and failure to thrive. All but one of the patients (patient 6) had a WAS score of 5. The patients' clinical characteristics are summarized in Supplementary Table 1.

Hematopoietic stem/progenitor cell engineering and transplantation. Autologous hematopoietic stem/progenitor cells (HSPCs) were transduced *ex vivo* with the LV-w1.6 WASp self-inactivating lentiviral vector²³ and immediately reinfused without cryopreservation, as described previously²⁰. The graft was collected from mobilized peripheral blood ($n=4$) or bone marrow ($n=4$) (Supplementary Table 1). At the time of gene therapy, the median patient age was 5.25 years (range, 0.8–30 years). The median vector copy number (VCN) per CD34⁺ cell in the drug product was 0.91 (range, 0.6–2.8). All of the patients underwent non-myeloablative conditioning with busulfan and fludarabine, as described previously²⁰, together with anti-CD20 therapy in one patient (patient 7). The median dose of CD34⁺ cells infused was 7.05×10^6 (range, $2-15 \times 10^6$) per kilogram of body weight. No serious adverse events were recorded during or after the cell infusion. Neither delayed neutrophil recovery nor a requirement for granulocyte colony-stimulating factor was observed after transplantation.

Clinical outcomes after gene therapy. After gene therapy, the patients were regularly evaluated over a period of at least 4 years. At the time of this interim analysis (cut-off, 1 October 2020), the median follow-up was 7.6 years (range, 4–9 years). The patients' clinical outcomes are summarized in Supplementary Table 1 and Extended Data Fig. 1.

The progressive reconstitution of hematopoietic lineages in all of the patients was accompanied by a reduction in the frequency and severity of infections. Patient 7 had fluctuating reactivation of

Epstein–Barr virus infection, but this was already present before gene therapy and did not require treatment. All of the patients discontinued their pre-gene therapy anti-infection prophylaxis, except for penicillin after splenectomy (and following myeloablative chemotherapy for UK patients). Five patients (patients 4, 5, 6, 8 and 9) discontinued immunoglobulin replacement therapy between 12 and 24 months after gene therapy. Eczema manifestations resolved in all but one patient (patient 7), who nevertheless had a marked reduction in the severity of eczema, with a decrease in the SCORing Atopic Dermatitis score²⁴ from 52 to 15.

Prior to gene therapy, all of the patients had severe microthrombocytopenia, in some cases associated with life-threatening episodes of cerebral or gastrointestinal bleeding (patients 2, 4, 5, 7 and 9). After gene therapy, none of the patients had spontaneous, severe bleeding despite below-normal platelet counts and none required platelet transfusions.

Patient 8 was treated at the age of 30 years. After gene therapy, autoimmune manifestations, inflammatory manifestations and infections were markedly less frequent. He was able to discontinue immunoglobulin replacement therapy and immunosuppressants and showed protective levels of post-vaccination antibody titers. Immune reconstitution and gene marking levels were stable. Four years after gene therapy, this splenectomized patient died of concomitant pneumococcal sepsis and H1N1 influenza.

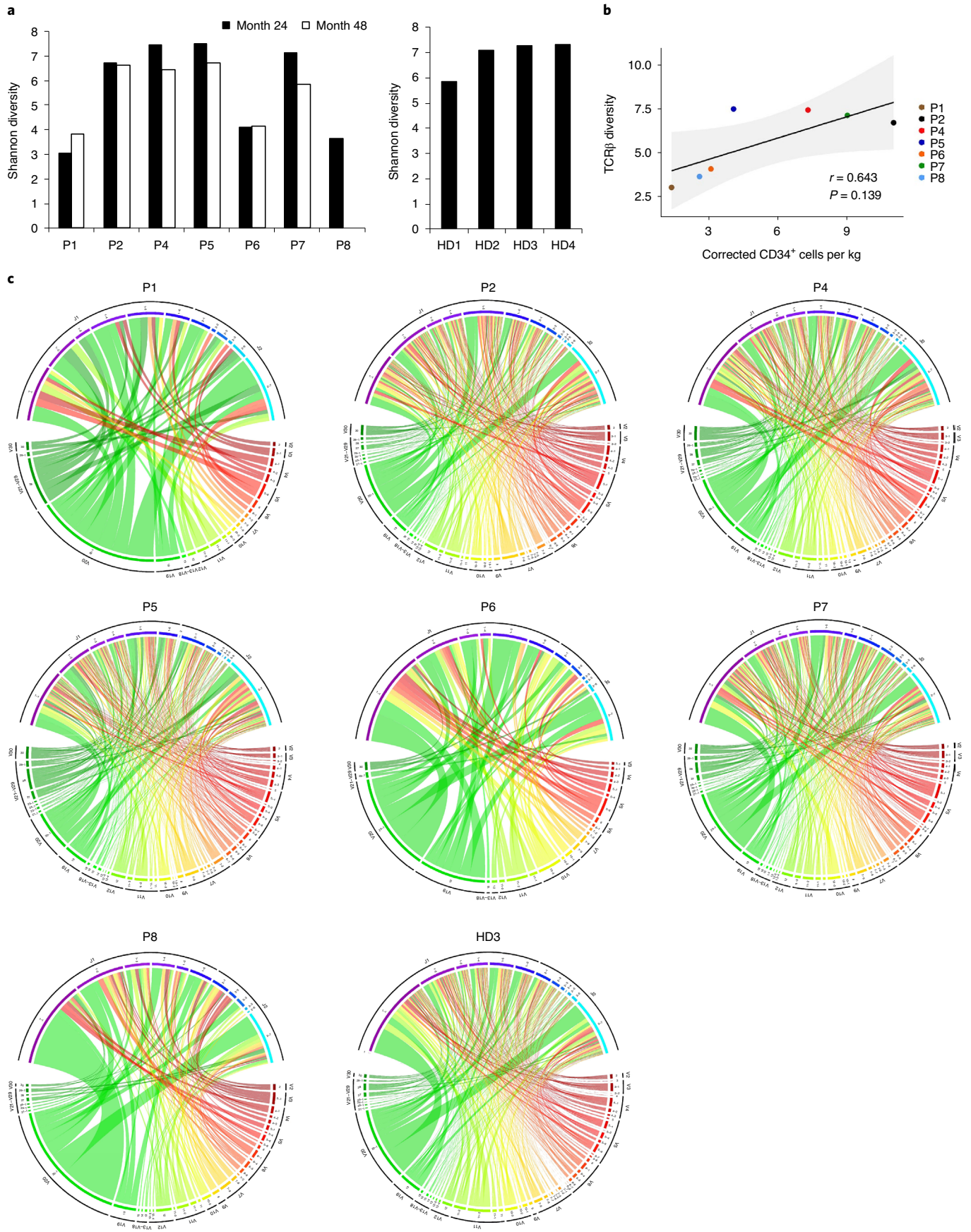
Patient 9 was treated at the age of 11 months. Twenty-one months after gene therapy, he presented with hematuria, proteinuria and edema. He was diagnosed with nephrotic syndrome, and a renal biopsy showed mild diffuse mesangial proliferative glomerulonephritis, immune complex-mediated. He was successfully treated with steroids, rituximab and mycophenolate mofetil. He is no longer taking immunosuppressants and is in good health.

With regard to inflammatory manifestations, patient 2 had developed very debilitating lower extremity vasculitis before gene therapy, which required wheelchair use. He underwent gene therapy at 16 years of age, followed by a marked improvement in vasculitis. He recovered the ability to walk but still had sequelae, including relapsing–remitting episodes of pain that partially responded to non-steroidal anti-inflammatory drugs and immunoglobulin replacement therapy. A marked improvement was observed after treatment with the human interleukin-1 receptor antagonist anakinra (100 mg per day); this treatment is ongoing and well tolerated.

Patient 4 had a single episode of single-joint (knee) inflammation 5 years after gene therapy, but recovered fully after conventional treatment with anti-inflammatory drugs. Three years later, he presented with moderate swelling of the ankles after an influenza vaccination, but this fully resolved after a short steroid treatment.

Myeloid reconstitution after gene therapy. All of the patients had stable engraftment in the first 3 weeks after gene therapy. The level of gene marking in CD15⁺ and CD14⁺ myeloid cells reached a median of 8.9% (range, 1–100%) after 4 years of follow-up and corresponded to the level of gene marking in the engrafted CD34⁺ HSPCs in the bone marrow (Extended Data Fig. 2a). Except in patient 9, this level did not increase further over time and was markedly lower than in the drug product (Extended Data Fig. 2b). The level of gene marking in CD15⁺ cells tended to correlate with the number of corrected CD34⁺ cells per kilogram infused (Extended Data Fig. 2c).

Fig. 2 | TCR β repertoire analysis. **a**, Shannon diversity of the TCR β clonotypes analyzed in patients with WAS (P1, P2, P4–P8) at months 24 and 48 of post-gene therapy follow-up (left) and in four healthy donors (HD1–HD4) (right). **b**, The Spearman correlation between the TCR β Shannon diversity at month 24 and the number of corrected CD34⁺ cells infused per kilogram, for each patient. The *P* value was calculated using the two-sided Spearman's rank correlation test, and *r* is Spearman's rank correlation coefficient. A regression line is represented in black and the 95% confidence interval is shown in gray. **c**, Circos plots showing V-gene and J-gene combinations in the repertoires analyzed in patients with WAS at month 48 of post-gene therapy follow-up (except for P8, shown at month 24) and in one healthy donor (HD3). The colored arcs define distinct V β and J β genes. The ribbon thickness is proportional to the frequency of a given combination.



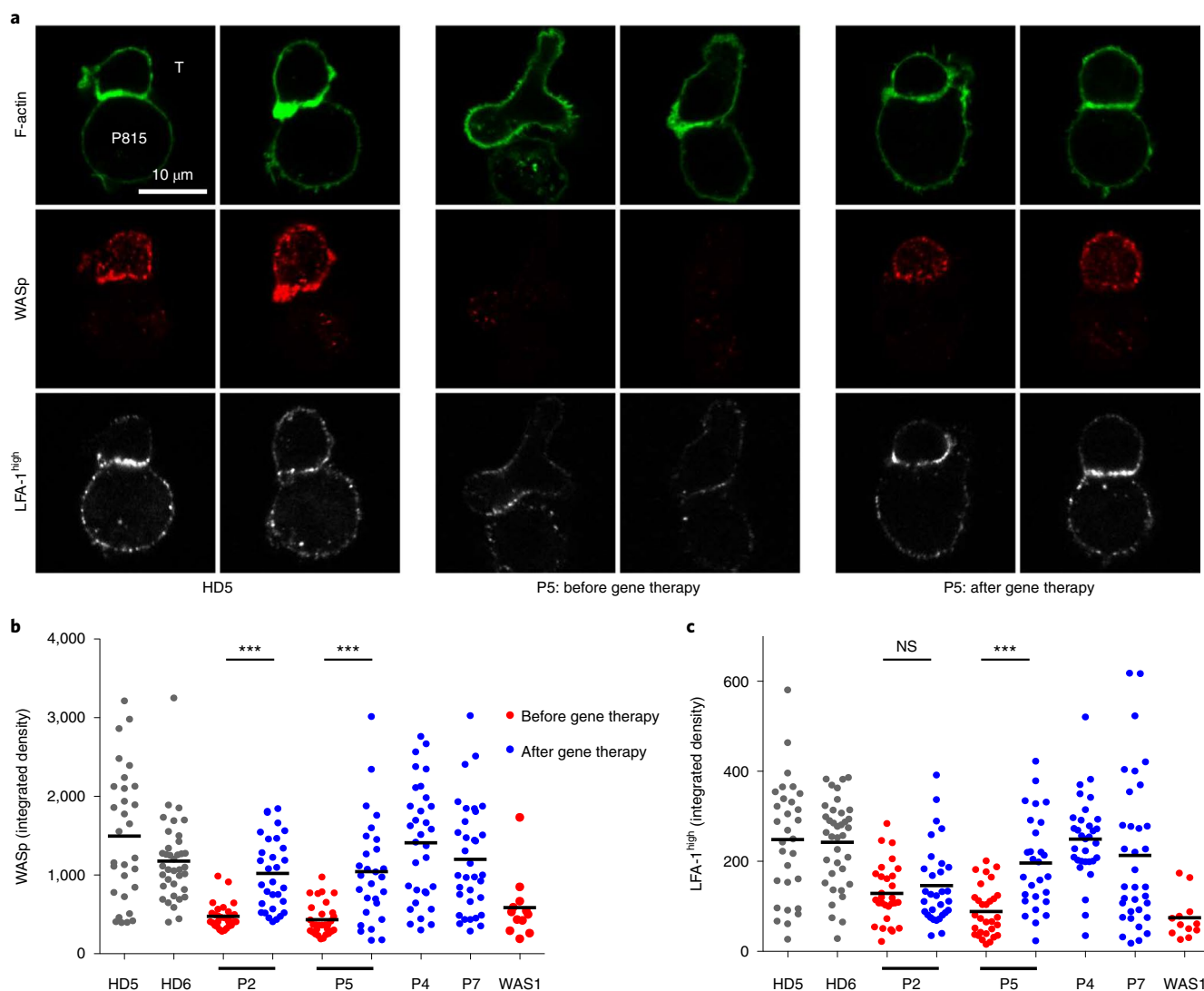


Fig. 3 | Restoration of T cell immune synapse assembly after gene therapy. **a**, Representative confocal microscopy images of conjugates between the indicated T cells (T, upper cells) and monoclonal anti-CD3 antibody-coated P815 cells (P815, lower cells), after staining for F-actin, WASp and high-affinity LFA-1. The T cells from P5 were collected 55 months after gene therapy; comparable data were collected from additional patients before and after gene therapy (P2) or after gene therapy (P4 and P7). The data were reproduced in two independent experiments (including cell preparation, staining and image acquisition). **b**, Integrated fluorescence density for WASp in T cells forming conjugates with monoclonal anti-CD3 antibody-coated P815 cells in patients with WAS before and after gene therapy (43, 55, 48 and 41 months afterwards for P2, P5, P4 and P7, respectively), in HDs (HD5 and HD6), and in one non-treated patient with WAS (WAS 1). **c**, Integrated fluorescence density for high-affinity LFA-1 in the same cells as in **b**. Overall, 28–37 conjugates per sample were analyzed. Similar results were obtained in another independent experiment. Statistical significance was assessed by unpaired t-test (two-tailed) ($***P < 0.0001$); NS, not significant ($P = 0.3866$). Black horizontal lines in **b** and **c** represent the mean.

T cell immune reconstitution after gene therapy. In all of the treated patients, the T cell counts increased over time and reached normal age-matched reference values (Fig. 1 and Extended Data Fig. 3). A gradual enrichment in WASp-positive CD3⁺ T cells demonstrated the proliferative and functional advantage of gene-corrected cells over non-corrected cells (Fig. 1). In all of the patients, the naive T cell and signal joint T cell receptor excision circle (sjTREC) counts were similar to those observed in age-matched controls, highlighting active thymopoiesis (Extended Data Fig. 4a–c). Using next-generation sequencing (NGS), the polyclonal T cell antigen receptor-beta (TCR β) repertoire was analyzed in seven patients 24 and 48 months after gene therapy (Fig. 2). The repertoire diversity was similar to that observed in healthy donors, except for in the three patients (patients 1, 6 and 8) who received the lowest dose of gene-corrected HSPCs (Fig. 2a). The TCR β repertoire diversity was correlated with the number

of corrected HSPCs per kilogram infused (Fig. 2b); it was stable, and no clonal expansion was detected (Fig. 2c).

To gain further insights into the functional recovery of the T cell compartment, we characterized the immune synapse in expanded T cells from four patients after gene therapy and compared these post-gene therapy data with the pre-gene therapy data, when available (Fig. 3). As shown for a representative patient in Fig. 3, confocal microscopy assessment of T cells forming conjugates with monoclonal anti-CD3 antibody-coated P815 cells showed that the immune synapse assembly was aberrant before gene therapy. The WASp-deficient T cells were elongated, lacked F-actin enrichment at the contact area and featured various types of actin-rich protrusions outside the contact area. Furthermore, the intensity of high-affinity lymphocyte function-associated antigen-1 (LFA-1) staining was lower than for control cells. After gene therapy, the T cells expressed

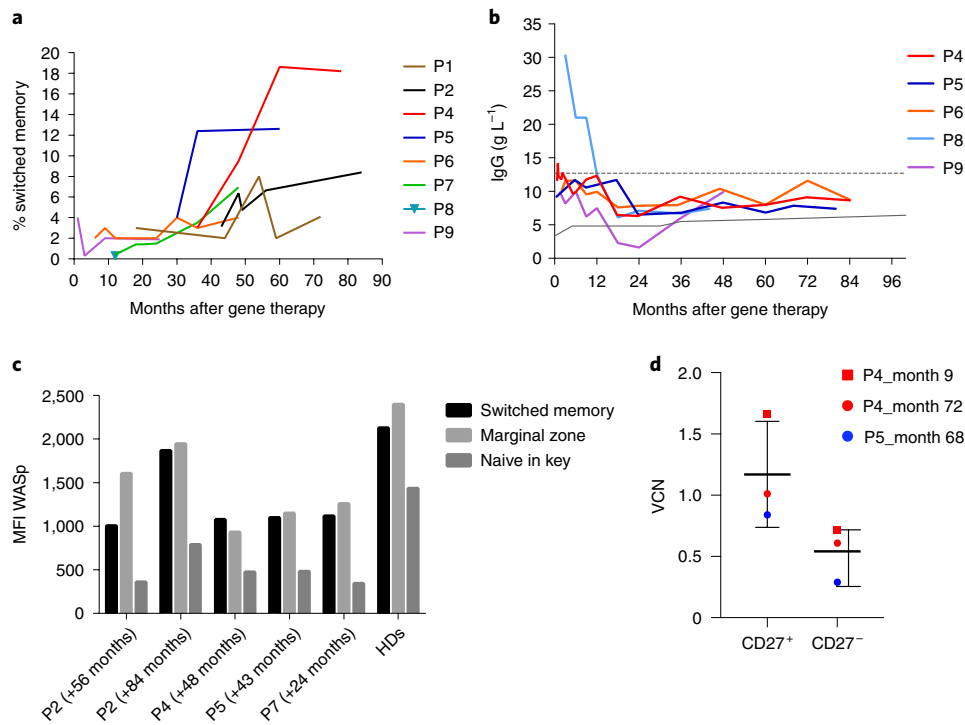


Fig. 4 | B cell reconstitution after gene therapy. **a**, Switched memory B cell subsets over time. **b**, IgG production in patients who discontinued intravenous immunoglobulin replacement therapy. Age-matched reference values are indicated by the gray lines (solid line, lower value; dashed line, upper value). **c**, WASp expression (mean fluorescence intensity (MFI) in arbitrary units) in switched memory, marginal zone and naive B cell subsets in patients (P) and healthy donors (HD7–HD11). **d**, The VCN in memory B cell (CD27⁺) and naive B cell (CD27⁻) subsets ($n=3$ biologically independent samples). Data are presented as the mean \pm s.e.m.

WASp at levels similar to those in healthy donors. WASp was located in the cytoplasm, with enrichment in the synapse (as seen in healthy donors). The post-gene therapy T cells had normalized immune synapse features, including the cell shape, F-actin enrichment and intensity of high-affinity LFA-1 (except in patient 1's T cells, in which the intensity of high-affinity LFA-1 remained low).

Overall, T cell compartment analysis documented robust immune reconstitution after gene therapy, which was associated with sustained clinical benefit.

B cell immune reconstitution after gene therapy. The B cell count increased progressively over time after gene therapy and reached age-matched reference values in all of the patients at last follow-up (Fig. 1). An enrichment in WASp-positive B cells was observed at the last follow-up, relative to baseline. This enrichment demonstrated the advantage of gene-corrected B cells over non-corrected cells, albeit to a lesser extent than for T cells. Accordingly, kappa-deleting recombination excision circle (KREC) counts, indicative of B cell neogenesis, were in the normal range (Extended Data Fig. 4d). Phenotype analysis showed progressive normalization of the distribution of different subsets in the B cell compartment, with an increase in the switched memory B cell subset in particular (Fig. 4a). No expansion of the CD21^{low}CD38^{low} B cell subset (including autoreactive B cells) was observed when compared with in-house reference values from healthy donors. The immunoglobulin production level increased progressively over time: the IgA levels reached age-matched reference values in all treated patients, although IgM levels remained below normal in four patients (Extended Data Fig. 5). At the time of our previous report²⁰, only two patients (patients 4 and 5) had been able to discontinue immunoglobulin replacement therapy. Since then, three additional patients (patients 6, 8 and 9) have discontinued immunoglobulin replacement and had normal levels of IgG

production (Fig. 4b). When available, the presence of protective levels of post-vaccination antibodies was highlighted (patients 4, 5 and 8; Supplementary Table 2). Patient 2 remains on immunoglobulin replacement therapy for the sequela of vasculitis, as described above.

For four patients, we were able to analyze WASp expression in the B cell subsets after gene therapy and compare it with the level in healthy donors (Fig. 4c). All of the patients had a greater proportion of WASp-expressing cells in the B cell memory subsets (including switched (CD19⁺CD27⁺IgD⁻) and marginal zone (CD19⁺CD27⁺IgD⁺) B cells) than in naive B cells (CD19⁺CD27⁻IgD⁺); this was confirmed by a greater mean fluorescence intensity for WASp in the memory subsets than in the naive cells. These patterns of WASp expression in B cell subsets were also observed in healthy donors ($n=5$) analyzed concomitantly. To further characterize these subsets, we analyzed the VCN in sorted memory (CD19⁺CD27⁺) and naive (CD19⁺CD27⁻) B cells. We observed significantly greater gene marking in memory B cells than in naive B cells (Fig. 4d). Furthermore, we compared the transduction level in subpopulations (when available) sorted concomitantly from peripheral blood and from bone marrow samples after gene therapy. We observed higher VCN levels in B cells from peripheral blood than in B cells from bone marrow, which suggests that gene-corrected B cells have a selective advantage after egress from the bone marrow (Extended Data Fig. 2a).

To investigate laboratory variables related to autoimmune features, samples collected before and after gene therapy were compared with regard to a panel of circulating autoantibodies. Before gene therapy, anti-nuclear antibodies (ANAs) were detected in all of the patients tested. Remarkably, the ANA titers after gene therapy were null or insignificant. Patient 2, who initially presented with very severe lower extremity vasculitis, presented with anti-RNP, anti-SmB, anti-SSA Ro and anti-SSB antibodies before

but not after gene therapy (Supplementary Table 3). Circulating and platelet-bound antiplatelet auto- and alloantibodies were studied separately (only after gene therapy) and were detected in patients 2, 4 and 7 (Supplementary Table 4).

Taken as a whole, these data suggest that gene therapy is able to correct the B cell compartment in WAS, with evidence for a selective advantage over time for genetically corrected B cells.

Platelet homeostasis and function after gene therapy. After gene therapy, platelet count increased over time and reached values of more than 140,000 platelets per μl at last follow-up in three patients (Fig. 5). These include patients 1 and 8, in whom thrombocytopenia was stably corrected after splenectomy (at 36 months after gene therapy and before gene therapy, respectively), and patient 9 (the patient with the highest engraftment of gene-corrected myeloid cells). For the other patients, the platelet count remained significantly below the normal range: from 20,000 to 50,000 platelets per μl for patients 2, 4 and 6 and below 20,000 platelets per μl for patients 5 and 7 (Fig. 5a and Extended Data Fig. 6a). Patient 2 had a splenectomy before gene therapy at the age of 8 years. This led to a temporary increase in the platelet count (up to 80,000 platelets per μl), followed by fluctuations and the observation of accessory spleen on ultrasound (Extended Data Fig. 7). For all of the patients, the platelet count 3 years after gene therapy tended to correlate with the level of gene marking in CD15⁺ cells (Fig. 5b). Patients (including those with below-normal platelet counts) did not present with spontaneous bleeding after gene therapy and no longer required platelet transfusions. Patients 4 and 7 received preventive platelet transfusions prior to scheduled surgery (7 years and a few months after gene therapy, respectively). Following a family decision, patient 5 started treatment with eltrombopag, a thrombopoietin receptor agonist (TRA), 6 years after gene therapy, without significant improvement in the platelet count. Six and a half years after gene therapy, patient 7 presented with a drop in the platelet count (5,000 platelets per μl) and developed cutaneous and mucosal ecchymosis. Treatment with the TRA romiplostim was initiated and led to a moderate increase in the platelet count (up to 34,000 platelets per μl).

To better characterize the platelets after gene therapy, a detailed functional and phenotypic analysis was performed on four patients from the same center (Necker-Enfants Malades Hospital). Platelet size was evaluated using flow cytometry, which is more accurate than automated blood cell counting, especially for small platelets. The results for the patients treated with gene therapy were compared with those for healthy donors and non-treated patients with WAS. We found that the platelets of the patients treated with gene therapy were larger than those of the non-treated patients with WAS but were still smaller than those of healthy donors (Fig. 5c). Moreover,

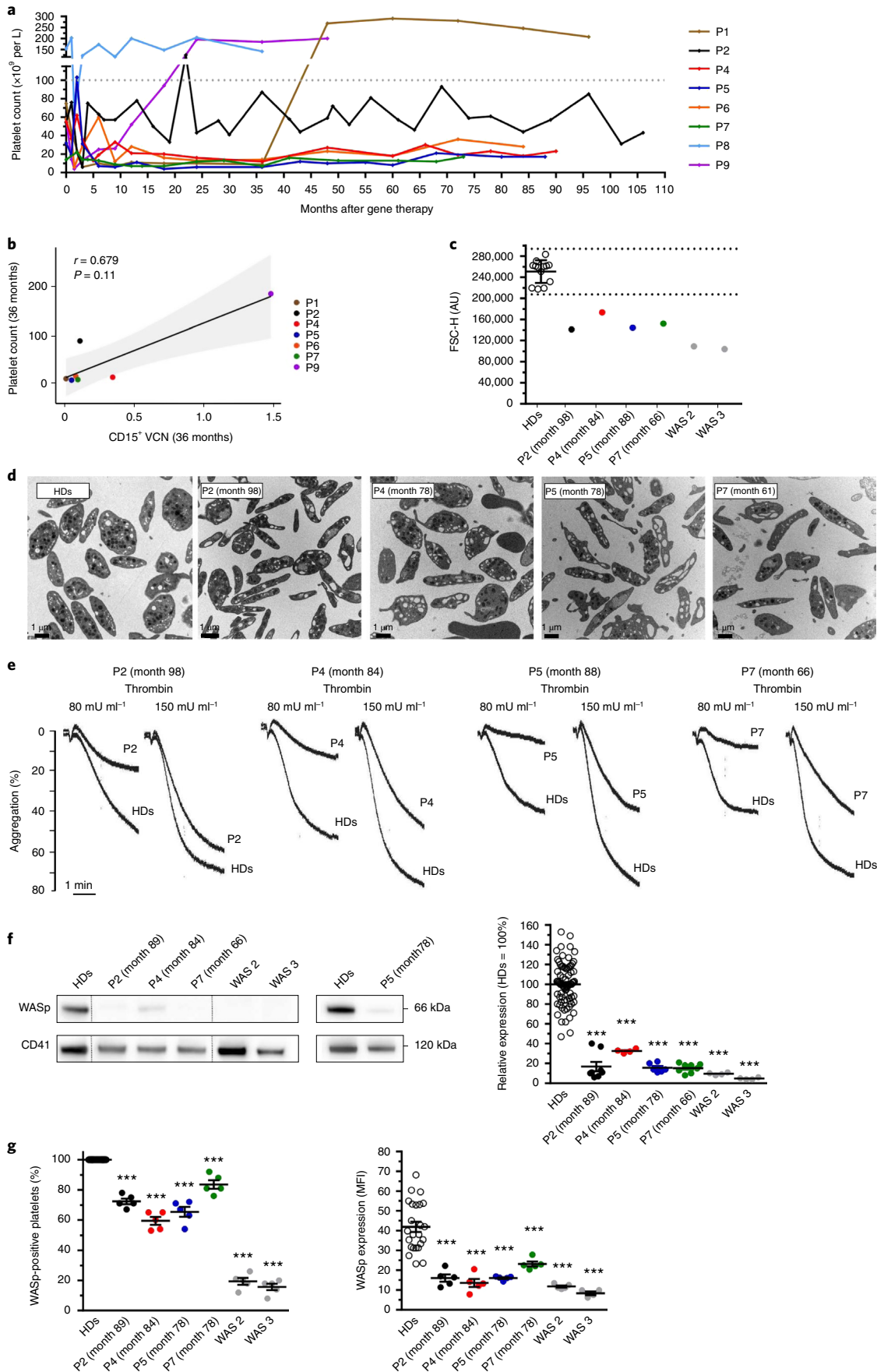
transmission electron microscopy ultrastructure analysis showed that the platelets of the patients treated with gene therapy were elongated; this contrasted with the disk-like shape of resting platelets from healthy donors (Fig. 5d and Extended Data Fig. 6b). The α -granule density was also slightly lower than normal, due to the smaller cell size (Extended Data Fig. 6c). To further evaluate hemostasis and platelet function after gene therapy, we studied the aggregation of washed platelets (Fig. 5e). At a low thrombin concentration (80 mU ml^{-1}), all of the patients had severe defects in platelet aggregation compared with healthy donors. Aggregation was less abnormal at a higher thrombin concentration (150 mU ml^{-1}), which suggests a partially functional response to agonist. Similar results were also observed after activation with adenosine diphosphate (ADP) (Extended Data Fig. 6d). To further evaluate the degree of platelet correction, WASp expression was evaluated using western blotting (Fig. 5f). All of the patients treated with gene therapy had suboptimal WASp expression (15–32% of that measured in healthy donors). The level of WASp expression after gene therapy was nevertheless higher than that observed in non-treated patients with WAS (5–10% of healthy donor values).

Next, we used an immunofluorescence assay to quantify WASp expression (Extended Data Fig. 6e) in individual platelets and to estimate the percentage of WASp-positive platelets and the level of WASp expression per platelet (Fig. 5g). The proportion of WASp-positive platelets ranged from 60% to 84% in the patients treated with gene therapy and from 16% to 19% in non-treated patients with WAS (Fig. 5g, left). It must be noted, however, that one of the two non-treated patients harbored a mutation resulting in residual WASp expression. However, the level of WASp expression per platelet in the gene therapy-treated patients was significantly lower (by 45–67%, $P < 0.001$) than in healthy donors (Fig. 5g, right). This indicates that, although a relatively high proportion of platelets re-expressed WASp after gene therapy, the level of WASp expression in individual platelets remained suboptimal. Last, antiplatelet antibodies were found in patients 2, 4 and 7 after gene therapy, as mentioned above.

Taken as a whole, these platelet measurements show that the gene therapy procedure only partially corrected the platelet compartment. However, this suboptimal recovery benefited the patients and was sufficient to prevent episodes of spontaneous hemorrhage.

Integration site and replication-competent lentivirus analyses. Vector integration site analysis of peripheral blood mononuclear cells (PBMCs) from the eight patients revealed a diversity of integration sites, with between 169 and 15,691 different sites (as analyzed using Illumina sequencing; Extended Data Fig. 8a). We observed high, time-stable values of the Pielou diversity index (a normalized version of the Shannon diversity index) for integration sites in the various patients^{25,26} (Extended Data Fig. 8b), reflecting successful

Fig. 5 | Hemostasis and platelet profile after gene therapy. **a**, Change over time in the platelet count for each patient after gene therapy. **b**, The Spearman correlation between platelet count and the level of gene marking (VCN) in CD15⁺ neutrophils after 3 years of follow-up for each patient (apart from P8, for whom the platelet count was corrected following splenectomy before gene therapy). The P value was calculated using the two-sided Spearman's rank correlation test, and r is Spearman's rank correlation coefficient. A regression line is represented in black and the 95% confidence interval is shown in gray. **c**, Platelet size, evaluated using flow cytometry. Each dot represents the mean size of washed platelets from healthy donors (HDs; $n = 13$), gene therapy-treated patients (P) and non-treated patients with WAS (WAS 2 and WAS 3). The results are expressed as the mean forward scatter height (FSC-H) \pm s.d. and the dotted lines indicate the normal range (mean \pm 2 s.d.). AU, arbitrary units. **d**, Platelet ultrastructure, which was analyzed once for each patient using transmission electron microscopy. **e**, The thrombin-induced aggregation of washed platelets was evaluated once for each patient (P) and healthy controls (HDs). Dotted lines indicate that the samples were derived from the same gel but are non-contiguous. The graph shows the mean of WASp expression \pm s.e.m. after normalization against CD41 expression from several independent experiments (HDs, $n = 82$; P4, WAS 2, WAS 3, $n = 4$; P5, $n = 6$; and P2, P7, $n = 8$). **f**, WASp expression was evaluated by immunofluorescence in platelets spread onto a fibrinogen matrix after activation with 20 μM ADP. The dot plot on the left shows the mean of the percentage \pm s.e.m. of platelets expressing WASp, and the dot plot on the right shows the mean of the WASp expression (determined from the MFI per platelet) \pm s.e.m. for five fields of view, which represent a total number of analyzed platelets of 816 for HDs, 170 for P2, 196 for P4, 175 for P5, 145 for P7, 158 for WAS 2 and 168 for WAS 3. In **f** and **g** statistical significance was determined using one-way analysis of variance with Dunnett's post test for multiple comparisons. In **f** (right) and **g** (left), the exact P value was $P < 0.0001$ for all of the patients, and in **g** (right) the exact P value was $P < 0.0001$ for P2, P4, P5, WAS 2, WAS 3 and $P = 0.0007$ for P7. In **c–g**, all HDs were different donors, except in **g** (left and right) where HDs were the same.



polyclonal gene correction. An analysis of the most abundant clones over time also highlighted strong, stable polyclonal reconstitution (Extended Data Fig. 8c), with no concerning clonal expansion. The monitoring of replication-competent lentivirus occurrence that was conducted as part of the human immunodeficiency virus (HIV) mRNA evaluation has been consistently negative at all time points tested in all of the present patients.

Discussion

We have previously reported preliminary data on seven patients with WAS who were treated with gene therapy and whose follow-up ranged from 9 to 42 months²⁰. In this updated report, we provide a comprehensive long-term analysis of data from the longest follow-up reported to date, with a median of 7.6 years (range, 4–9 years), and include two additional patients treated since the last report. The present study confirms our earlier results and provides additional evidence of the long-term efficacy of gene therapy for WAS, as well as the safety track record. Here, sustained multilineage engraftment of gene-modified cells was observed in the peripheral blood and the bone marrow. In turn, this led to increasing expression of WASp in the patients' cells and clinical resolution of severe eczema and susceptibility to recurrent infections. In line with these results, T cell function was restored, as shown by the recovery of immune synapse assembly and normal naive T cell count and functions after gene therapy. The T cell compartment was reconstituted in the patient treated at the age of 30 years, suggesting that gene therapy for WAS is also a treatment option in adult patients²², despite the continuing risk associated with splenectomy²⁷.

In parallel with the robustness of T cell reconstitution, a normalized B cell compartment was observed, in line with previous studies^{28,29}, as shown in particular by the increasing level of WASp⁺ switched memory B cells over time and the age-matched level of KRECs. Five patients were able to discontinue prophylactic antibiotic treatment and immunoglobulin replacement therapy while achieving normal post-vaccination antibody titers. The level of gene marking was greater in lymphoid than in myeloid cells. This is consistent with the strong proliferative and/or survival advantage conferred by WASp expression in the lymphoid compartment, as predicted by earlier observations in mice and in patient cells^{30,31}. This was also reported in the WAS gene therapy trial conducted in Milan with the same vector²¹.

No graft failure or treatment-related adverse events were observed after gene therapy. Vector integration site analyses showed that the insertion profile was safe and diverse, with no concerning clonal expansion.

In the present study, we focused on two major concerns in patients with WAS: thrombocytopenia and autoimmunity. The mechanisms of thrombocytopenia in WAS include defective central thrombocytopoiesis and increased peripheral destruction^{32–34}. A recent study has highlighted functional and phenotypic abnormalities and an altered proteomic profile in WASp-deficient platelets³⁴. This senescent profile accelerates the peripheral destruction of platelets. After gene therapy, the patients had a marked decrease in the frequency and severity of spontaneous bleeding episodes. Platelet count increased over time and reached more than 140,000 platelets per μl in three patients (that is, two splenectomized patients and the patient with the strongest engraftment of gene-corrected myeloid cells). Platelet count in the other patients remained subnormal, perhaps because of the low WASp expression in this lineage or the residual autoimmunity in some patients, as recently described in a conditional mouse model³³. Given that the gene marking level in the myeloid lineage reflects the engraftment of corrected HSCs in the bone marrow, one can propose that the initial quantity of HSCs infused and the level of gene marking in the cell product influence the recovery of platelet count. A higher level of gene correction might also improve the migration of true stem cells into the bone marrow. The low degree of

myeloid chimerism, despite adequate VCN and HSC counts in the infused drug product, might also be due to the defective migration of WASp^{low} HSCs described previously³⁵.

After gene therapy, a few autoimmune manifestations were observed: persistence of lower extremity vasculitis (in patient 2), new nephrotic syndrome occurrence (in patient 9) and presence of antiplatelet antibodies (in patients 2, 4 and 7). The level of circulating autoantibodies detected before gene therapy (including ANA and vasculitis-related autoantibodies) was normalized after treatment. Further improvement in autoimmune features after gene therapy might result from the inclusion of an anti-CD20 agent in the conditioning regimen.

The main difference with the results from the Milan trial^{19–21} concerned platelet count. The count was below the normal range in both studies but lower in the present patients. This disparity might be due to differences in the severity score and age of the treated patients and in the VCN of the infused drug product. Disease prior to gene therapy was more severe in the present trial than in the Milan trial, as evidenced by the median Zhu score (5 versus 4, respectively). Moreover, the present patients were older at the time of gene therapy than those in the Milan trial (median age of 5.25 years versus 2.2 years, respectively). Last, the median VCN was lower in the present trial than in the Milan trial (0.9 versus 2.4, respectively).

Further lentiviral vector optimization (with a stronger promoter, for example) has been considered as a possible means of enhancing WASp levels in platelets^{36–38}. Alternatively, enhancement of the ex vivo transduction procedure might usefully result in higher levels of gene correction of WAS HSPCs in terms of both cell frequency and the VCN.

In conclusion, gene therapy is a safe, efficacious treatment for patients with WAS who lack a suitable HSCT donor. More efficacious and more reliable transduction protocols and conditioning regimens are likely to improve outcomes further, particularly with regard to platelet recovery, for which the advantages of intrinsic correction are less apparent.

Online content

Any methods, additional references, Nature Research reporting summaries, source data, extended data, supplementary information, acknowledgements, peer review information; details of author contributions and competing interests; and statements of data and code availability are available at <https://doi.org/10.1038/s41591-021-01641-x>.

Received: 29 January 2021; Accepted: 24 November 2021;

Published online: 24 January 2022

References

- Thrasher, A. J. & Burns, S. O. WASP: a key immunological multitasker. *Nat. Rev. Immunol.* **10**, 182–192 (2010).
- Candotti, F. Clinical manifestations and pathophysiological mechanisms of the Wiskott-Aldrich syndrome. *J. Clin. Immunol.* **38**, 13–27 (2018).
- Albert, M. H., Notarangelo, L. D. & Ochs, H. D. Clinical spectrum, pathophysiology and treatment of the Wiskott-Aldrich syndrome. *Curr. Opin. Hematol.* **18**, 42–48 (2011).
- Zhu, Q. et al. The Wiskott-Aldrich syndrome and X-linked congenital thrombocytopenia are caused by mutations of the same gene. *Blood* **86**, 3797–3804 (1995).
- Imai, K. et al. Clinical course of patients with WASP gene mutations. *Blood* **103**, 456–464 (2004).
- Mahloufi, N. et al. Characteristics and outcome of early-onset, severe forms of Wiskott-Aldrich syndrome. *Blood* **121**, 1510–1516 (2013).
- Dupuis-Girod, S. et al. Autoimmunity in Wiskott-Aldrich syndrome: risk factors, clinical features, and outcome in a single-center cohort of 55 patients. *Pediatrics* **111**, 622–627 (2003).
- Ozsahin, H. et al. Long-term outcome following hematopoietic stem-cell transplantation in Wiskott-Aldrich syndrome: collaborative study of the European Society for Immunodeficiencies and European Group for Blood and Marrow Transplantation. *Blood* **111**, 439–445 (2008).

9. Moratto, D. et al. Long-term outcome and lineage-specific chimerism in 194 patients with Wiskott-Aldrich syndrome treated by hematopoietic cell transplantation in the period 1980-2009: an international collaborative study. *Blood* **118**, 1675–1684 (2011).
10. Shin, C. R. et al. Outcomes following hematopoietic cell transplantation for Wiskott-Aldrich syndrome. *Bone Marrow Transplant.* **47**, 1428–1435 (2012).
11. Elfeky, R. A. et al. One hundred percent survival after transplantation of 34 patients with Wiskott-Aldrich syndrome over 20 years. *J. Allergy Clin. Immunol.* **142**, 1654–1656 (2018).
12. Burroughs, L. M. et al. Excellent outcomes following hematopoietic cell transplantation for Wiskott-Aldrich syndrome: a PIDTC report. *Blood* **135**, 2094–2105 (2020).
13. Balashov, D. et al. A conditioning regimen with plerixafor is safe and improves the outcome of TCR α^+ and CD19 $^+$ cell-depleted stem cell transplantation in patients with Wiskott-Aldrich syndrome. *Biol. Blood Marrow Transplant.* **24**, 1432–1440 (2018).
14. Wada, T. et al. Second-site mutation in the Wiskott-Aldrich syndrome (WAS) protein gene causes somatic mosaicism in two WAS siblings. *J. Clin. Invest.* **111**, 1389–1397 (2003).
15. Davis, B. R. et al. Somatic mosaicism in the Wiskott-Aldrich syndrome: molecular and functional characterization of genotypic revertants. *Clin. Immunol.* **135**, 72–83 (2010).
16. Trifari, S. et al. Revertant T lymphocytes in a patient with Wiskott-Aldrich syndrome: analysis of function and distribution in lymphoid organs. *J. Allergy Clin. Immunol.* **125**, 439–448 (2010).
17. Braun, C. J. et al. Gene therapy for Wiskott-Aldrich syndrome: long-term efficacy and genotoxicity. *Sci. Transl. Med.* **6**, 227ra33 (2014).
18. Cavazzana, M., Bushman, F. D., Miccio, A., André-Schmutz, I. & Six, E. Gene therapy targeting haematopoietic stem cells for inherited diseases: progress and challenges. *Nat. Rev. Drug Discov.* **18**, 447–462 (2019).
19. Aiuti, A. et al. Lentiviral hematopoietic stem cell gene therapy in patients with Wiskott-Aldrich syndrome. *Science* **341**, 1233151 (2013).
20. Hacein-Bey Abina, S. et al. Outcomes following gene therapy in patients with severe Wiskott-Aldrich syndrome. *JAMA* **313**, 1550–1563 (2015).
21. Ferrua, F. et al. Lentiviral haematopoietic stem/progenitor cell gene therapy for treatment of Wiskott-Aldrich syndrome: interim results of a non-randomised, open-label, phase 1/2 clinical study. *Lancet Haematol.* **6**, 239–253 (2019).
22. Morris, E. C. et al. Gene therapy for Wiskott-Aldrich syndrome in a severely affected adult. *Blood* **130**, 1327–1335 (2017).
23. Dupré, L. et al. Lentiviral vector-mediated gene transfer in T cells from Wiskott-Aldrich syndrome patients leads to functional correction. *Mol. Ther.* **10**, 903–915 (2004).
24. Stalder, J. F. et al. Severity scoring of atopic dermatitis: the SCORAD index. Consensus report of the European Task Force on Atopic Dermatitis. *Dermatology* **186**, 23–31 (1993).
25. Pielou, E. C. The measurement of diversity in different types of biological collections. *J. Theor. Biol.* **13**, 131–144 (1966).
26. Ramezani, H. A note on the normalized definition of Shannon's diversity index in landscape pattern analysis. *Environ. Nat. Resources Res.* **2**, 54–60 (2012).
27. Rivers, E., Worth, A., Thrasher, A. J. & Burns, S. O. Bleeding and splenectomy in Wiskott-Aldrich syndrome: a single-centre experience. *J. Allergy Clin. Immunol. Pract.* **7**, 1042–1044 (2019).
28. Pala, F. et al. Lentiviral-mediated gene therapy restores B cell tolerance in Wiskott-Aldrich syndrome patients. *J. Clin. Invest.* **125**, 3941–3951 (2015).
29. Castiello, M. C. et al. B-cell reconstitution after lentiviral vector-mediated gene therapy in patients with Wiskott-Aldrich syndrome. *J. Allergy Clin. Immunol.* **136**, 692–702 (2015).
30. Rengan, R. et al. Actin cytoskeletal function is spared, but apoptosis is increased, in WAS patient hematopoietic cells. *Blood* **95**, 1283–1292 (2000).
31. Westerberg, L. S. et al. WASP confers selective advantage for specific hematopoietic cell populations and serves a unique role in marginal zone B-cell homeostasis and function. *Blood* **112**, 4139–4147 (2008).
32. Sabri, S. et al. Deficiency in the Wiskott-Aldrich protein induces premature proplatelet formation and platelet production in the bone marrow compartment. *Blood* **108**, 134–140 (2006).
33. Sereni, L. et al. Autonomous role of Wiskott-Aldrich syndrome platelet deficiency in inducing autoimmunity and inflammation. *J. Allergy Clin. Immunol.* **142**, 1272–1284 (2018).
34. Sereni, L. et al. Lentiviral gene therapy corrects platelet phenotype and function in patients with Wiskott-Aldrich syndrome. *J. Allergy Clin. Immunol.* **144**, 825–838 (2019).
35. Charrier, S. et al. Wiskott-Aldrich syndrome protein-deficient hematopoietic cells can be efficiently mobilized by granulocyte colony-stimulating factor. *Haematologica* **98**, 1300–1308 (2013).
36. Muñoz, P. et al. WAS promoter-driven lentiviral vectors mimic closely the lopsided WASP expression during megakaryocytic differentiation. *Mol. Ther. Methods Clin. Dev.* **19**, 220–235 (2020).
37. Astrakhan, A. et al. Ubiquitous high-level gene expression in hematopoietic lineages provides effective lentiviral gene therapy of murine Wiskott-Aldrich syndrome. *Blood* **119**, 4395–4407 (2012).
38. Singh, S. et al. Safe and effective gene therapy for murine Wiskott-Aldrich syndrome using an insulated lentiviral vector. *Mol. Ther. Methods Clin. Dev.* **4**, 1–16 (2016).

Publisher's note Springer Nature remains neutral with regard to jurisdictional claims in published maps and institutional affiliations.



Open Access This article is licensed under a Creative Commons Attribution 4.0 International License, which permits use, sharing, adaptation, distribution and reproduction in any medium or format, as long as you give appropriate credit to the original author(s) and the source, provide a link to the Creative Commons license, and indicate if changes were made. The images or other third party material in this article are included in the article's Creative Commons license, unless indicated otherwise in a credit line to the material. If material is not included in the article's Creative Commons license and your intended use is not permitted by statutory regulation or exceeds the permitted use, you will need to obtain permission directly from the copyright holder. To view a copy of this license, visit <http://creativecommons.org/licenses/by/4.0/>.

© The Author(s) 2022, corrected publication 2022

¹Department of Biotherapy, Hôpital Universitaire Necker-Enfants Malades, Groupe Hospitalier Paris Centre, Assistance Publique-Hôpitaux de Paris, Paris, France. ²Biotherapy Clinical Investigation Center, Groupe Hospitalier Universitaire Paris Centre, Assistance Publique-Hôpitaux de Paris, INSERM CIC 1416, Paris, France. ³Clinical Investigation Center CIC 1419, Hôpital Universitaire Necker-Enfants Malades, Groupe Hospitalier Paris Centre, Université de Paris, Assistance Publique-Hôpitaux de Paris, Paris, France. ⁴INSERM, UMR_S1176, Université Paris-Saclay, Le Kremlin-Bicêtre, France. ⁵Department of Paediatric Immunology, Great Ormond Street Hospital, London, UK. ⁶Molecular and Cellular Immunology Section, UCL Great Ormond Street Institute of Child Health, London, UK. ⁷Toulouse Institute for Infectious and Inflammatory Diseases (INFINITY), INSERM, CNRS, Toulouse III Paul Sabatier University, Toulouse, France. ⁸Ludwig Boltzmann Institute for Rare and Undiagnosed Diseases, Vienna, Austria. ⁹Department of Dermatology, Medical University of Vienna, Vienna, Austria. ¹⁰Institute of Immunity and Transplantation, University College London, London, UK. ¹¹Department of Immunology, Royal Free London Hospitals NHS Foundation Trust, London, UK. ¹²Laboratoire d'Hématologie, Assistance Publique-Hôpitaux de Paris, Hôpital Necker-Enfants Malades, Paris, France. ¹³EMiLy, INSERM U1160, Institut de Recherche Saint Louis, Université de Paris, Paris, France. ¹⁴Laboratoire d'Immunologie et d'Histocompatibilité, Hôpital Saint-Louis, Assistance Publique-Hôpitaux de Paris, Paris, France. ¹⁵Institut Necker-Enfants Malades (INEM), INSERM U1151, Université Paris Descartes Sorbonne Cité, Paris, France. ¹⁶Laboratory of Onco-Hematology, Assistance Publique-Hôpitaux de Paris, Necker-Enfants Malades University Hospital, Paris, France. ¹⁷Département d'Immunologie, Groupement Hospitalier Pitié-Salpêtrière, Assistance Publique-Hôpitaux de Paris, Paris, France. ¹⁸Centre d'Immunologie et des Maladies Infectieuses-Paris (CIMI-Paris), INSERM, Sorbonne Université, Paris, France. ¹⁹Platelet Immunology Department, INTS, Paris, France. ²⁰Department of Pediatric Immunology, Hematology and Rheumatology, Assistance Publique-Hôpitaux de Paris, Necker-Enfants Malades University Hospital, Paris, France. ²¹Imagine Institute, Université Paris Centre, Paris, France. ²²Human Lymphohematopoiesis Laboratory, Imagine Institute, INSERM UMR 1163, Université de Paris, Paris, France. ²³Service d'Hématologie Adultes, Hôpital Necker-Enfants Malades, Assistance Publique-Hôpitaux de Paris, Centre Université de Paris, Paris, France. ²⁴Department of Microbiology, University of Pennsylvania School of Medicine, Philadelphia, PA, USA. ²⁵Unité des Technologies Chimiques et Biologiques pour la Santé, CNRS, INSERM, Université de Paris, Paris, France. ²⁶Clinical Immunology Laboratory, Groupe Hospitalier Universitaire Paris-Sud, Hôpital Kremlin-Bicêtre, Assistance Publique-Hôpitaux de Paris, Le Kremlin-Bicêtre, France. ²⁷Généthon, Evry, France. ²⁸Study Center for Primary Immunodeficiencies, Assistance Publique-Hôpitaux de Paris, Necker-Enfants Malades University Hospital, Paris, France. ²⁹Integrare Research Unit UMR_S951, Université Paris-Saclay, Université d'Evry, Inserm, Genethon, Evry, France. ³⁰Collège de France, Paris, France. ³¹These authors contributed equally: A. Magnani, M. Semeraro. ³²These authors jointly supervised this work: A. Fischer, E. Six, A. J. Thrasher, M. Cavazzana. ✉e-mail: a.thrasher@ucl.ac.uk; m.cavazzana@aphp.fr

Methods

Study design and patient enrollment. We have previously reported on a non-randomized, open-label, phase I/II clinical study (based on a lentiviral gene therapy vector) involving seven pediatric patients with severe WAS. Details of the gene therapy study design and procedures have been reported previously²⁰. The patients were treated at Necker-Enfants Malades Hospital (Paris, France; ClinicalTrials.gov identifier [NCT01347346](#)) and at Great Ormond Street Hospital (London, UK; ClinicalTrials.gov identifier [NCT01347242](#)). Patients were enrolled in the Long Term Safety Follow up of Haematopoietic Stem Cell Gene Therapy for the Wiskott–Aldrich Syndrome (WASFUP) study (ClinicalTrials.gov identifier [NCT02333760](#)), which was designed to follow patients for an additional 13 years after the initial gene therapy study. The WASFUP study protocol was approved by the UK and French drug regulatory agencies and the appropriate investigational review boards, such as the Gene Therapy Advisory Committee in the United Kingdom and the Comité de Protection des Personnes in France. A CONSORT flow diagram detailing enrollment of the patients is available in the Supplementary Information. Data were collected manually and transferred to the Altizem Society for data management through Clintrial software.

The primary endpoint for the initial WAS trials ([NCT01347346](#) and [NCT01347242](#)) was to assess the efficacy of HSC gene therapy in patients with WAS, based on clinical improvement in at least one of the following parameters (depending on the patient symptom profile at study entry): eczema status, the frequency and severity of infections, bruising and bleeding episodes, and autoimmune disorders and the number of disease-related days of hospitalization. The three secondary objectives were to assess the safety of HSC gene therapy in patients with WAS, the efficacy of HSC gene therapy for the progression of microthrombocytopenia and the need for its treatment, and the efficacy for other hematological variables, including WASp expression and reconstitution of humoral and cell-mediated immunity.

The eligibility criteria were male sex (any age); severe WAS (clinical score 3–5) or absence of WASp in PBMCs determined on western blotting and flow cytometry; molecular confirmation using WAS gene DNA sequencing; lack of HLA-genotypically identical bone marrow or 10/10 or 9/10 antigen HLA-matched unrelated donor or HLA-matched cord blood after a 3-month search; signed informed consent or assent by the parent, guardian or patient; willingness to return for follow-up (only for patients who have received previous allogeneic HSCT); failed allogeneic HSCT; and contraindication to repeat transplantation.

The exclusion criteria were HLA-genotypically identical bone marrow; 10/10 or 9/10 antigen HLA-matched unrelated donor or HLA-matched cord blood; contraindication to leukapheresis; contraindication to bone marrow harvest; contraindication to conditioning medication; and HIV positivity.

The six primary endpoints for the long-term safety follow-up trial ([NCT02333760](#)) were the incidence and type of serious adverse events and, more specifically, the incidence and nature of delayed events (such as malignancies, hematologic events, autoimmune events and mortality continuously for the duration of the post-gene therapy follow-up study); the safety of the gene therapy procedure for gene transfer analysis at yearly post-gene therapy visits (lentiviral integration sites in different cell subpopulations, quantification of the VCN in sorted cell populations using real-time quantitative PCR); the safety of the gene therapy procedure with regard to the absence of replication-competent lentiviruses (RCLs) at yearly post-gene therapy visits; the change in medical conditions; the key medical events related to WAS (eczema status, infections, bleeding symptoms, autoimmune manifestation); and the hematological and cell-mediated and humoral immunity reconstitution. The three secondary endpoints were change in the need for associated treatments at the yearly post-gene therapy visit (immunoglobulin replacement therapy, antibacterial, antifungal and antiviral drugs, transfusions etc.); the representation of TCR families using PCRs, TREC assays and the TCR V β panel after gene therapy; and bone marrow integrity (optional) after gene therapy via bone marrow aspiration. The WASFUP study ([NCT02333760](#)) was designed as a longitudinal descriptive study without interim analysis. It has included nine eligible and consenting patients between October 2014 and November 2019. Considering the duration of the study (13 years), an intermediate evaluation of the majority of primary and secondary endpoints (delayed events, key medical events, biological parameters of vector expression and insertion, RCL, platelet and immune reconstitution), as well as additional exploratory investigations on T cells and platelets, was conducted for the first eight patients having at least 4 years of follow-up after gene therapy. These eight patients described here were included in the WASFUP study between 29 October 2014 and 13 December 2015. Some prespecified biological and medical parameters of the WASFUP study were not reported, such as duration of hospital stay, humoral or cellular responses to antigens, and bone marrow exploration, given that the clinical study is still ongoing. The two inclusion criteria were enrollment in the initial phase I/II WAS trial conducted in France and the United Kingdom and signed informed consent by the parents, guardians or patients. The only exclusion criterion was unwillingness in parents, guardians or patients to return for the follow-up study period.

Written informed consent or assent was obtained after the benefits and risks of the trial had been explained to the patients or their parents or legal guardians. The study was carried out in accordance with the tenets of the Declaration of Helsinki.

Patients were included in the present study if they had at least 4 years of follow-up. One patient (patient 3) died 7 months after gene therapy from pre-existing complications of infection, as reported previously²⁰, and was therefore not included in the present study. Since the initial report, two additional patients treated at Great Ormond Street Hospital have been followed for at least 4 years after gene therapy and so were included in the present study (patients 8 and 9). Data were obtained from blood samples provided by patients with WAS after gene therapy (patients 1–9) at routine hospital visits and were compared with data from blood samples from non-treated patients with WAS (WAS 1–3) and adult healthy donors (healthy donors 1–11). Blood samples from healthy individuals were obtained from the French Blood Establishment (Etablissement Français du Sang (EFS); ref: C CPSP UNT-N°18/EFS/031, and collection DC-2015-2488 approved by the ethics board Comité de Protection des Personnes CPP Sud Ouest et Outre-Mer II (France)) and from adult healthy volunteers upon informed consent, in accordance with the tenets of the Declaration of Helsinki; the study participants were informed about the anonymous use of their personal data. Patient WAS 1 corresponds to patient WAS 2 (male, 5 years) in the 2002 study by Dupré et al.³⁹. This patient carries a 2-nucleotide deletion (AG) in exon 4 (position 484–485) of the WAS gene resulting in a stop codon (codon 167). Patients WAS 2 and WAS 3 are currently followed at Necker-Enfants Malades Hospital in Paris; sampling was obtained during regular visits at the hospital, upon informed consent. Peripheral blood samples from these patients were obtained in accordance with the tenets of the Declaration of Helsinki (including informed consent). Published age-matched reference values were used for lymphoid subsets⁴⁰, neutrophils⁴¹ and immunoglobulins⁴². Internal age-matched reference values were generated and used for sjTRECs and sjKRECs (pediatric, $n = 20$; adult, $n = 199$). The CD21^{low}CD38^{low} B cell subset data for patients after gene therapy were compared with in-house reference values from healthy controls ($n = 30$) analyzed with the same gating strategy. The diagnosis of WAS was confirmed by genetic testing.

Outcomes. Since our initial report, we have regularly collected data on a range of clinical and laboratory variables: immune reconstitution, the VCN and WASp expression in sorted myeloid and lymphoid populations, and integration site profiles. T cell correction was evaluated using real-time quantitative PCR assays of sjTRECs, and the TCR repertoire was evaluated using NGS. In four patients, immune synapse assembly was studied before and after gene therapy. Platelet function and phenotype were comprehensively characterized for four gene therapy patients, non-treated patients with WAS and healthy donors. We recorded changes over time in B cell count and function, including subpopulation phenotype, WASp expression in B cell subsets, VCN in the memory (CD19⁺CD27⁺) and naive (CD19⁺CD27⁻) compartments, KRECs, immunoglobulin production and post-vaccination titer. Patients were tested for a panel of autoantibodies (including antiplatelet antibodies) before and after gene therapy, when possible. Age-matched reference values were added for the different immunological parameters, based on pediatric reference ranges^{40,41}.

Isolation of mononuclear cells. In line with the trial protocol, peripheral blood was sampled regularly during follow-up, while bone marrow was sampled once after gene therapy (unless required more frequently for medical reasons). Mononuclear cells were isolated from peripheral blood or bone marrow using standard Ficoll gradient separation. Lymphocyte subpopulations were studied using fluorochrome-coupled antibodies (BD Bioscience, Miltenyi Biotec), and the absolute lymphocyte count was determined using TruCount Tubes (BD Bioscience), as described previously²⁰.

Immunophenotyping and sorting of hematopoietic subpopulations. Cells were stained with specific, directly labeled monoclonal antibodies, according to the manufacturer's instructions and as described previously²⁰. An eight-color FACSCanto II cell analyzer and FACSAria II cell sorter (BD Biosciences) were used for flow cytometry analysis and cell sorting, respectively, according to the manufacturer's instructions. Flow cytometry data were analyzed using FlowJo software (TreeStar).

Proliferation assays. T cell lymphoproliferation was assayed by measuring the incorporation of tritiated thymidine in response to a challenge with phytohemagglutinin (Sigma-Aldrich) or tetanus toxoid (Staten), as described previously²⁰.

Clonogenic assay and DNA extraction. Erythroid burst-forming unit and granulocyte–macrophage colony-forming unit progenitors or precursors were grown in semisolid methylcellulose medium supplemented (or not) with erythropoietin (Methocult H4435 and H4535, respectively; STEMCELL Technologies), according to the manufacturer's instructions. Single colonies were picked for DNA extraction.

Gene marking. Gene marking in sorted subpopulations was monitored via VCN analysis, as described previously²⁰.

TREC and KREC analysis. sjTRECs and sjKRECs were quantified using a real-time PCR assay, as described previously⁴³. In brief, a 1:200 or 1:2,000 dilution

of an initial multiplex PCR amplification was quantified in duplicate for each of the different primer–probe sets on a ViiA7 Real-Time PCR System (Applied Biosystems).

sjTREC and sjKREC counts are given per 150,000 cells (around 1 µg DNA) after normalization against the albumin gene content. Data are expressed as the log₁₀ count per 150,000 PBMCs.

TCR repertoire analysis. To analyze the TCR repertoire, genomic DNA was extracted from blood samples or PBMCs. The TCRβ repertoire was assessed with one-step NGS using 100 ng DNA and EuroClonality-NGS amplicon primers⁴⁴. The DNA was sequenced on an Illumina MiSeq system, using 2 × 250-bp v2 chemistry. Figures were prepared with R software (<https://www.R-project.org/>). The Shannon diversity index was calculated using the vegan package. Circos plots showing the various V-gene and J-gene combinations were designed using the circlize package.

Detection of autoantibodies. Serum samples from all participants were screened for ANAs using HEp-2000TM commercial slides (Immunoconcept). HEp-2000TM cells are HEp-2 cells that overexpress Ro60 antigens. Serum samples were diluted 1:80 in PBS and incubated for 25 min at room temperature in a humid chamber. After two washes in PBS, cells were incubated with FITC-conjugated goat anti-human IgG (immunoglobulin heavy and light chains, Immunoconcept) for another 25 min in the dark. After two more washes in PBS, the slides were counterstained with Evans blue and assembled with glycerol and coverslips. Specific antibodies were detected using a multiplex ENA (extractable nuclear antigen) assay on the FIDIS instrument (Theradiag), an anti-DNA ELISA (DiaSorin), a Farr assay (Trinity Biotech) and/or an anti-nucleosome ELISA (Werfen). Samples were also screened for anti-neutrophil cytoplasmic antibodies (ANCA) using commercial NOVA LiteH ANCA ethanol or formalin slides. Thirty microliters of a sample diluted 1:20 was spotted on each well, incubated for 25 min and washed with PBS buffer (Immunoconcept). Cells were subsequently incubated with FITC-conjugated goat anti-human immunoglobulin for 25 min in the dark. After two washes in PBS, slides were counterstained with Evans blue and assembled with glycerol and coverslips. Indirect immunofluorescence screening for anti-tissue antibodies on triple rodent tissue (stomach, liver, kidney; Biosystems) was performed with IgG antibodies against smooth muscle, mitochondria, LKM1, parietal cells, LC1, SLA and intrinsic factor. Serum samples were diluted 20-fold in PBS and incubated for 30 min at room temperature in a moist chamber. After two washes in PBS, the slides were incubated with FITC-conjugated goat anti-human IgG, IgM and IgA antibodies. Slides were examined under a fluorescence microscope. To minimize subjective bias, two observers had to agree on the results of the ANCA assay, the ANA assay and the indirect immunofluorescence screening for anti-tissue antibodies.

Evaluation of T cell immune synapse assembly. T cells were expanded by stimulation of PBMCs with irradiated PBMCs and Epstein–Barr virus-immortalized B cells (JY cells), interleukin (IL)-2 (100 U ml⁻¹) and IL-15 (5 ng ml⁻¹) in RMPI medium containing 5% human serum. As an internal control, a T cell line derived from a previously described patient with WAS (referred to here as WAS1, corresponding to patient 2 in the report by Dupré et al.³⁹) was added to the samples from the gene therapy-treated patients. To rule out selection bias in the in vitro expansion step, we confirmed that the VCN at the time of immune synapse analysis was similar to that measured at sampling (median VCN, 1.29 and 1.15, respectively). Immune synapse assembly was evaluated as described previously⁴⁵ by mixing T cells with anti-CD3 monoclonal antibody (mAb) (10 µg ml⁻¹ OKT3, eBioscience)-coated P815 cells and depositing the resulting cell conjugates on poly(L-lysine)-coated slides with preformed reaction wells (Marienfeld). Unlabeled a24 mAb (Biolend) that binds to LFA-1 in its high-affinity conformation was added at a concentration of 2.5 µg ml⁻¹ for 10 min at 37 °C. The conjugates were then fixed, permeabilized and stained with phalloidin-AF488 (Invitrogen) and anti-WASp rabbit mAb (Abcam, ab75830). The anti-LFA-1 and anti-WASp antibodies were then visualized with anti-mouse AF647-coupled and anti-rabbit AF564-coupled secondary antibodies (Invitrogen), respectively. Slides were examined under an LSM-710 confocal microscope (×63/1.4 oil immersion Plan-Apochromat objective, Carl Zeiss). To calculate the integrated density of WASp and high-affinity LFA-1, images of randomly selected T cell:P815 cell conjugates were acquired and then analyzed with ImageJ software.

Platelet characteristics and function. *Preparation of washed platelets.* Venous blood from healthy donors or patients was collected in 10% ACD/A buffer (75 mM sodium citrate, 44 mM citric acid and 136 mM dextrose, pH 4.5). As described previously⁴⁶, platelets were washed in the presence of apyrase grade VII (100 mU ml⁻¹, Sigma-Aldrich) and prostaglandin E₁ (1 µM, Sigma-Aldrich) to minimize platelet activation. The platelet count was then adjusted to 3 × 10⁸ platelets per ml in Tyrode's buffer (137 mM NaCl, 2 mM KCl, 0.3 mM NaH₂PO₄, 1 mM MgCl₂, 5.5 mM glucose, 5 mM N-(2-hydroxyethyl)piperazine-N'-2-ethanesulfonic acid, 12 mM NaHCO₃ and 2 mM CaCl₂, pH 7.3).

Flow cytometry evaluation of platelet size. Platelet size was evaluated using a BD Accuri C6 flow cytometer (BD Biosciences) by recording the forward scatter parameters.

Platelet aggregation. Platelet aggregation was monitored by measuring light transmission through a stirred suspension of washed platelets (3 × 10⁸ platelets per ml) at 37 °C, using a Chrono-Log aggregometer (Chrono-Log), as described previously⁴⁷. Platelet aggregation was triggered by bovine thrombin (Sigma-Aldrich) and ADP.

Western blotting for WASp expression. Washed platelets (3 × 10⁸ platelets per ml) were lysed in Laemmli sample buffer (10 mM HEPES, 2% SDS, 10% glycerol, 5 mM EDTA). The proteins were reduced by incubation with 25 mM dithiothreitol, separated by electrophoresis using NuPage 4–12% Bis-Tris Protein gels (Invitrogen) and transferred to nitrocellulose membranes, which were incubated with mouse anti-WASp primary antibody (1 µg ml⁻¹, clone B-9; Santa Cruz) or mouse anti-CD41 (0.2 µg ml⁻¹, clone SZ22, used as a loading control for normalization; Beckman Coulter). Immunoreactive bands were visualized with enhanced chemiluminescence detection reagents (Perbio Science) and a G-BOX Chemi XT16 Image System and were then quantified using Gene Tools v4.03.05.0 (Syngene).

Immunofluorescence assay of WASp expression. Glass coverslips were coated with 100 µg ml⁻¹ human fibrinogen (HYPHEN BioMed SAS) in PBS (0.01 M H₂PO₄, 0.154 M NaCl, pH 7.4 ± 0.2) at 4 °C overnight and then blocked with 5% BSA. Washed platelets (3 × 10⁶) were stimulated with ADP (20 µM, to induce full platelet spreading; Sigma-Aldrich), plated on fibrinogen-coated glass coverslips and incubated for 30 min at 37 °C. After washing, platelets were fixed for 15 min with 4% paraformaldehyde, permeabilized with 0.2% Triton X-100, blocked with 1% BSA and stained with primary mouse anti-WASp antibody (4 µg ml⁻¹, clone B-9; Santa Cruz). The primary antibody was detected using a goat anti-mouse IgG Alexa Fluor 555 conjugate (4 µg ml⁻¹, Invitrogen), and platelet morphology was assessed by labeling cytoskeletal F-actin with Alexa Fluor 488-phalloidin (0.3 µM, Invitrogen). Last, the coverslips were mounted on slides, and immunofluorescence images were acquired on an epifluorescence microscope (Nikon, Eclipse 600). WASp expression was quantified using ImageJ.

Transmission electron microscopy. Washed platelets were fixed by incubation for 1 h at room temperature in 1.25% glutaraldehyde in 0.1 M phosphate buffer (pH 7.2), centrifuged for 10 min at 1,100g and washed once in 0.1 M phosphate buffer. Platelets were stored in 0.2% glutaraldehyde at 4 °C until processing for standard transmission electron microscopy analysis of platelet morphology, as described previously⁴⁸.

Detection of antiplatelet autoantibodies and/or alloantibodies. For each patient analyzed, 15 ml blood was collected in EDTA tubes for the detection of autoantibodies bound to platelet glycoprotein complexes. Serologic assays for circulating autoantibodies and/or alloantibodies were performed on 10 ml blood collected in dry tubes. Patients' antiplatelet antibodies were detected using monoclonal antibody-specific immobilization of platelet antigen technique, according to the manufacturer's instructions (apDia)⁴⁹.

Integration site analyses. Vector integration sites were amplified, sequenced and analyzed using the INSPIRED pipeline, as described previously^{50–52}. The Pielou diversity index (a normalized version of the Shannon diversity index) was calculated using the vegan package.

Statistical analysis. Results are reported as the mean ± s.d. or the median, unless stated otherwise. All statistical analyses were performed using GraphPad Prism6 (GraphPad). Data were analyzed using one-way analysis of variance followed by a post hoc test, as indicated in the figure legends. The threshold for statistical significance was set to *P* < 0.05. The statistical significance of the Spearman correlation between parameters was evaluated using the cor.test function in R software.

Reporting Summary. Further information on research design is available in the Nature Research Reporting Summary linked to this article.

Data availability

Data that support the findings in this study are available from the authors upon agreement of the sponsor (S.A., Genethon). Restriction may apply to the availability of these data before the end of the study as they are part of clinical trials, subject to patient confidentiality, and are not public. Integration site sequence data used in the present study are available in the NCBI Sequence Read Archive (SRA, reference nos. SRP050221 and PRJNA685802). TCR NGS sequence data and RCL analyses are available upon request. Source data are provided with this paper.

Code availability

Several functions and packages from R software (<https://www.R-project.org/>) have been used for analyses as mentioned in the specific sections.

References

- Dupré, L. et al. Wiskott-Aldrich syndrome protein regulates lipid raft dynamics during immunological synapse formation. *Immunity* **17**, 157–166 (2002).

40. Schatorjé, E. J. H. et al. Paediatric reference values for the peripheral T cell compartment. *Scand. J. Immunol.* **75**, 436–444 (2012).
41. Segel, G. & Halterman, J. Neutropenia in pediatric practice. *Pediatr. Rev.* **29**, 12–23 (2008).
42. Picard, C. Comment explorer un déficit immunitaire héréditaire? *Rev. Prat.* **57**, 1671–1676 (2007).
43. Arruda, L. C. M. et al. Immune rebound associates with a favorable clinical response to autologous HSCT in systemic sclerosis patients. *Blood Adv.* **2**, 126–141 (2018).
44. Brüggemann, M. et al. Standardized next-generation sequencing of immunoglobulin and T-cell receptor gene recombinations for MRD marker identification in acute lymphoblastic leukaemia; a EuroClonality-NGS validation study. *Leukemia* **33**, 2241–2253 (2019).
45. Houmadi, R. et al. The Wiskott-Aldrich syndrome protein contributes to the assembly of the LFA-1 nanocluster belt at the lytic synapse. *Cell Rep.* **22**, 979–991 (2018).
46. Adam, F., Verbeuren, T. J., Fauchère, J. L., Guillin, M. C. & Jandrot-Perrus, M. Thrombin-induced platelet PAR4 activation: role of glycoprotein ibandap. *J. Thromb. Haemost.* **1**, 798–804 (2003).
47. Adam, F. et al. Platelet JNK1 is involved in secretion and thrombus formation. *Blood* **115**, 4083–4092 (2010).
48. Berrou, E. et al. A mutation of the human *EPHB2* gene leads to a major platelet functional defect. *Blood* **132**, 2067–2077 (2018).
49. Kiefel, V., Santoso, S., Weisheit, M. & Mueller-Eckhardt, C. Monoclonal antibody-specific immobilization of platelet antigens (MAIPA): a new tool for the identification of platelet-reactive antibodies. *Blood* **70**, 1722–1726 (1987).
50. Sherman, E. et al. INSPIRED: a pipeline for quantitative analysis of sites of new DNA integration in cellular genomes. *Mol. Ther. Methods Clin. Dev.* **4**, 39–49 (2017).
51. Berry, C. C. et al. INSPIRED: quantification and visualization tools for analyzing integration site distributions. *Mol. Ther. Methods Clin. Dev.* **4**, 17–26 (2017).
52. Six, E. et al. Clonal tracking in gene therapy patients reveals a diversity of human hematopoietic differentiation programs. *Blood* **135**, 1219–1231 (2020).

Acknowledgements

The study was sponsored by Genethon (Evry France) and supported by funding from AFM/Telethon. The present work was also supported by grants from the European Research Council (ERC-2015-AdG, GENEFORCURE, project 693762), by state funding from the Agence Nationale de la Recherche under the Investissements d'avenir program (ANR-10-IAHU-01), and by the Paris Ile-de-France Region under the DIM Thérapie génique initiative. The project has also received funding from the European Union's Horizon 2020 research and innovation program under grant agreement 693762–Gene For Cure. A.J.T., C.B., J.X.B., R.E., C.R. and H.B.G. received support from the National Institute for Health Research Biomedical Research Centre at Great Ormond Street Hospital for Children NHS Foundation Trust (London, UK). A.J.T. was supported by the Wellcome Trust (104807/Z/14/Z and 217112/Z/19/Z). We thank the patients and their families for their cooperation in the study. We thank J. Marouene (study coordinator at Assistance Publique-Hôpitaux de Paris at the URC-CIC Paris Centre) for the study's implementation, monitoring and data management; A. Guilloux (LAMME, Evry University) for critical advice on statistical analysis; B. Beaurain, C. Colpin and C. Tran

at Genethon for management of the sponsor activities, study pharmacovigilance and regulatory affairs, respectively; D. Lasne and T. Pascreau at Necker Children's Hospital (Hematology Department, Paris) and C. Repérant (U1176 INSERM, Le Kremlin-Bicêtre) for their assistance with platelet studies; and the members of the Cytometry Facility at Necker Hospital and the Cell Imaging Facility at the Toulouse Institute for Infectious and Inflammatory Diseases. We also thank the CIQLE Laënnec-Centre d'Imagerie Quantitative Lyon-Est (France) for expert technical assistance with the electron microscopy studies, and we thank J. C. Bordet (Laboratoire d'Hémostase, Centre de Biologie Est, Hospices Civils de Lyon, Bron, France) for his expertise in transmission electron microscopy and image analysis.

Author contributions

M.C., A.F., A.J.T., C.B., M.S., E.C.M., D.M. and A.M. performed the transplantations, provided patient and family care, and monitored the patients; M.C., A.J.T., A.F., S.H.-B.-A., H.B.G., J.X.B., A. Galy, E.S., A.M., C.B., F.A. and C.L. designed the study and collected and analyzed the data; A.J.T., A.M., M.S., E. Magrin, F.S., C.B., R.E. and C. Rivat collected blood samples and clinical data; F.A., D.B. and A.K. analyzed platelets; C.P. analyzed immune reconstitution; A. Toubert and E.C. analyzed TRECs/KRECs; E. Macintyre, C.A., A.D. and A. Trinquand analyzed the TCR repertoire; L.D. and M.G. analyzed the T cell immune synapse; F.D.B., E.S., A.D., J.E. and A.M.R. analyzed the vector insertion site; G.G., M.M. and R.P. analyzed autoantibodies; C. Roudaut, A. Gabrion and M.G. isolated, stained and sorted cells, performed clonogenic assays, extracted DNA and provided technical support; M.C., A.M., E.S., F.A., L.D., A.D. and M.G. prepared figures and tables; M.C., A.M., E.S., L.D. and F.A. wrote the manuscript; M.S., A.F., L.D., A. Toubert, E.C., F.D.B., S.H.-B.-A. and F.A. critically reviewed the manuscript. M.C. and A.J.T. (the study's principal investigators on each site) acknowledge that they had full access to all the study data and take responsibility for the integrity of the data and the accuracy of the data analysis. The sponsor, as represented by A. Galy and S.A., has been involved in the design and conduct of the study; collection, management, analysis and interpretation of the data; preparation, review and approval of the manuscript; and decision to submit the manuscript for publication.

Competing interests

A.J.T. holds equity in Orchard Therapeutics. A. Galy and S.A. work at Genethon (sponsor). All other authors declare no competing interests.

Additional information

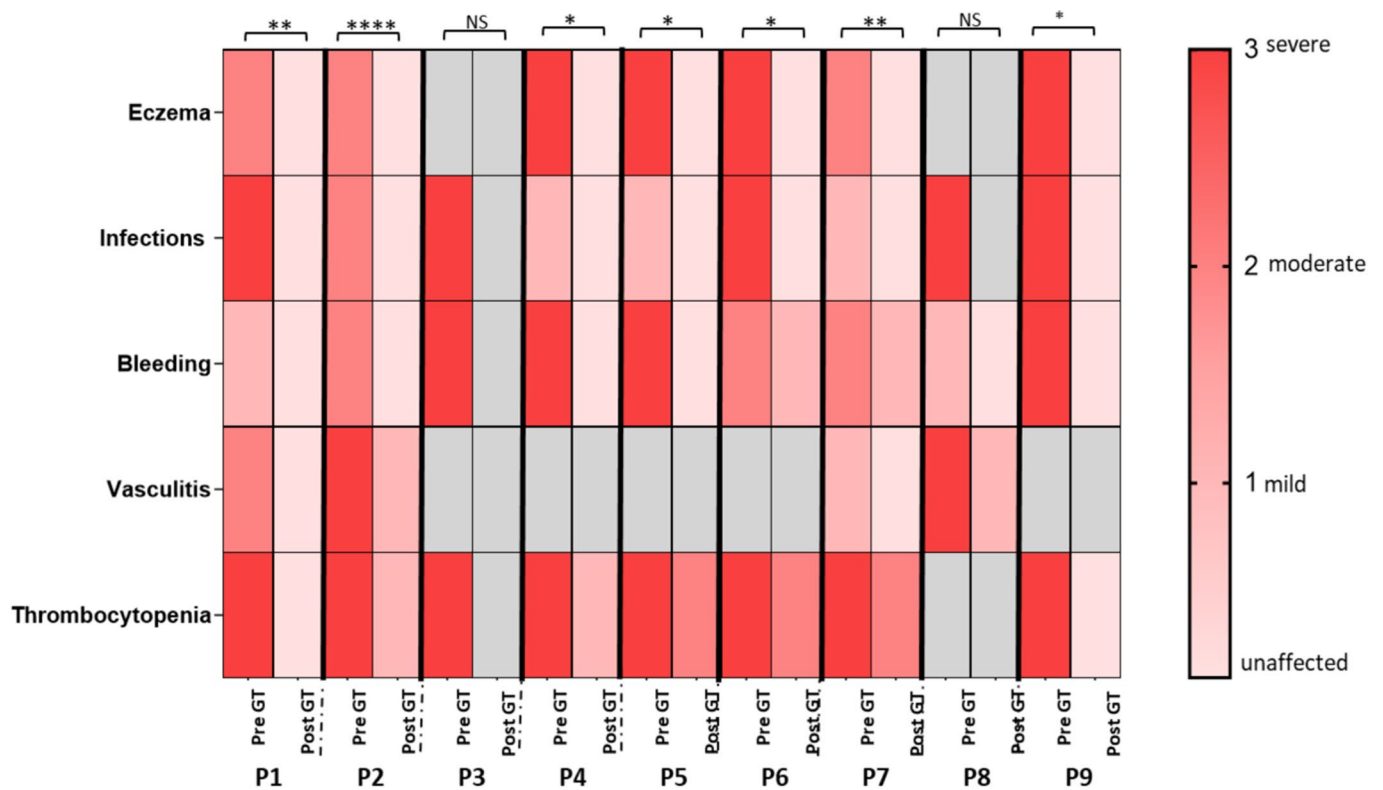
Extended data are available for this paper at <https://doi.org/10.1038/s41591-021-01641-x>.

Supplementary information The online version contains supplementary material available at <https://doi.org/10.1038/s41591-021-01641-x>.

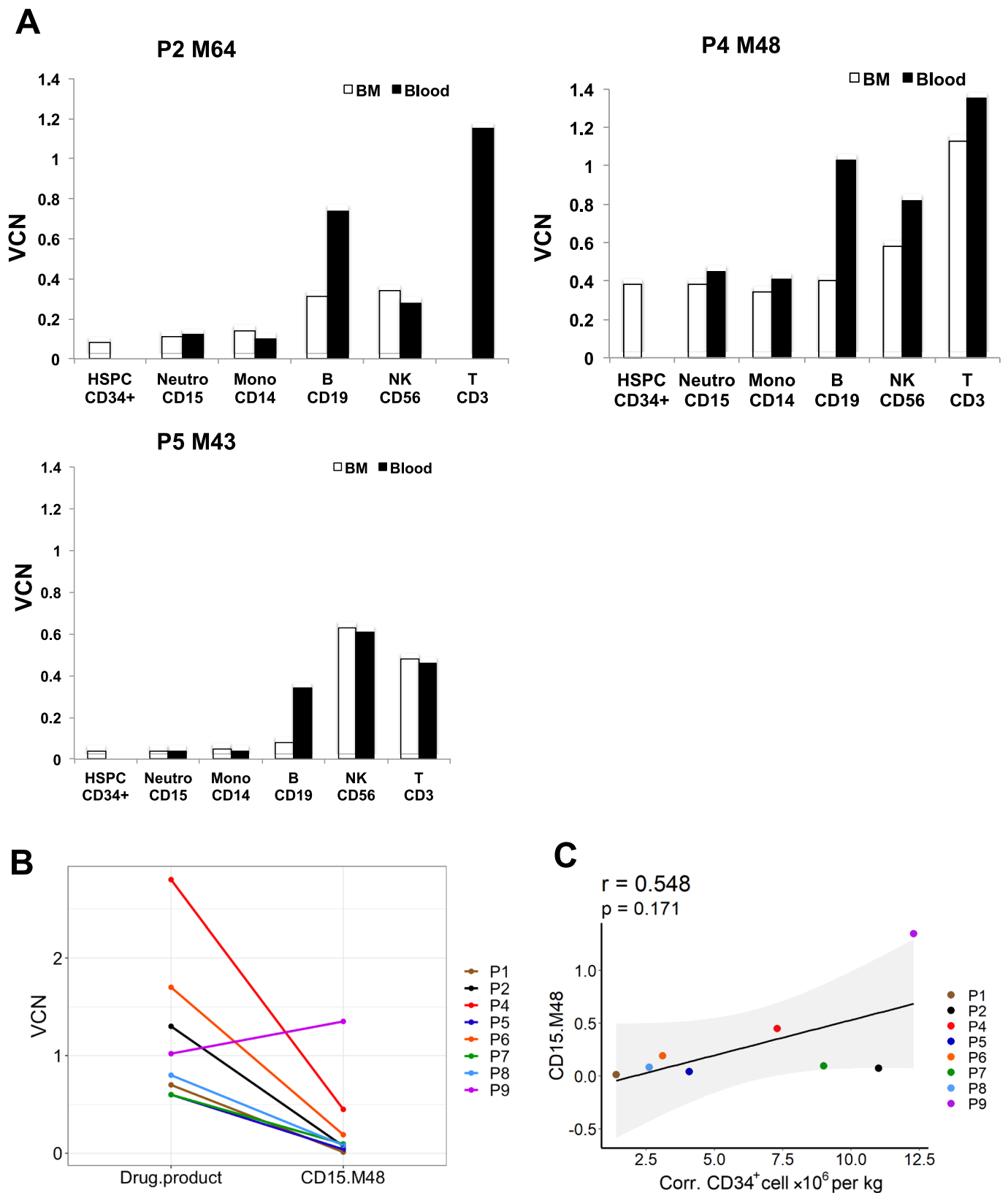
Correspondence and requests for materials should be addressed to A. J. Thrasher or M. Cavazzana.

Peer review information *Nature Medicine* thanks Alessandra Biffi, Jenna Bergerson and the other, anonymous, reviewer(s) for their contribution to the peer review of this work. Anna Maria Ranzoni was the primary editor on this article and managed its editorial process and peer review in collaboration with the rest of the editorial team.

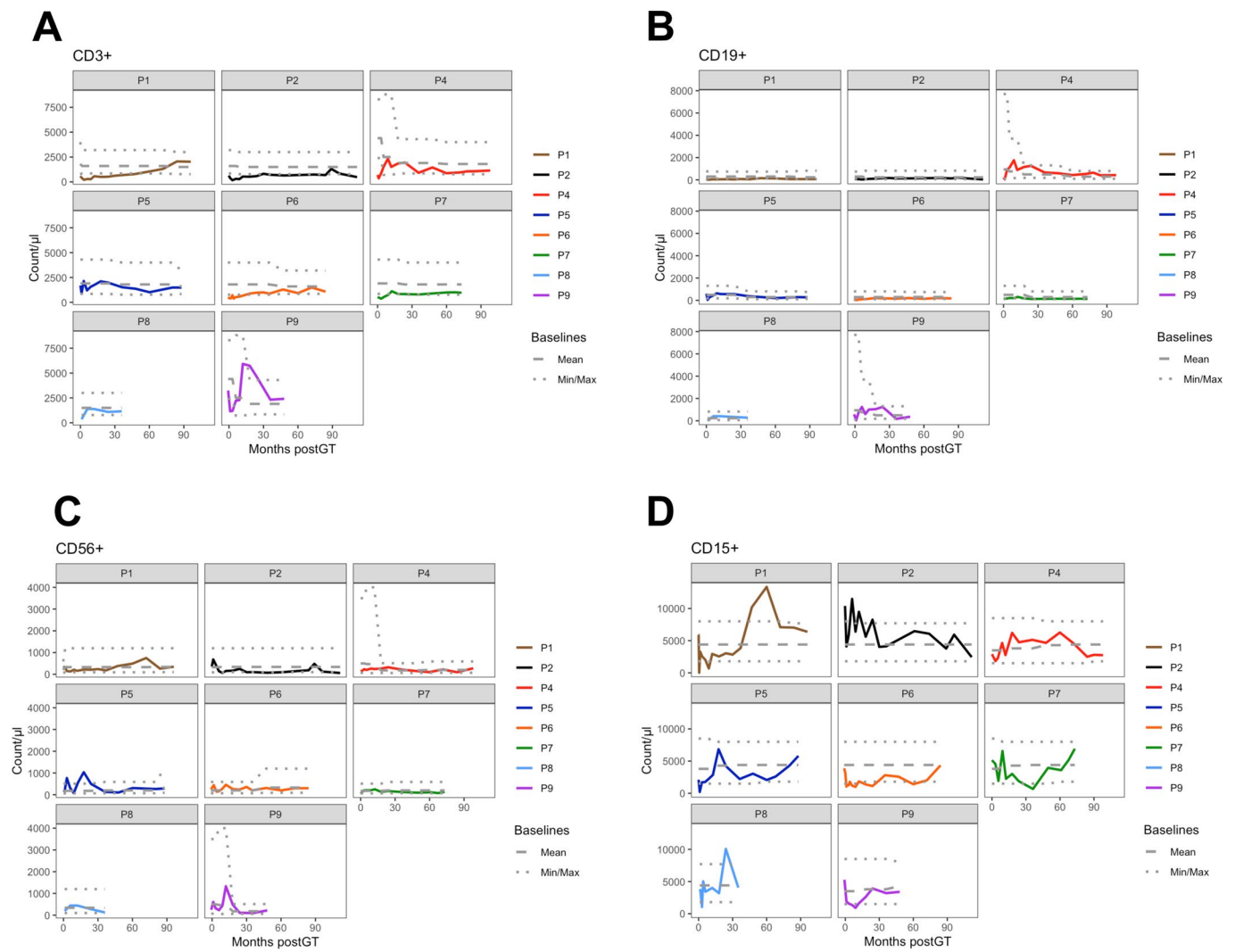
Reprints and permissions information is available at www.nature.com/reprints.



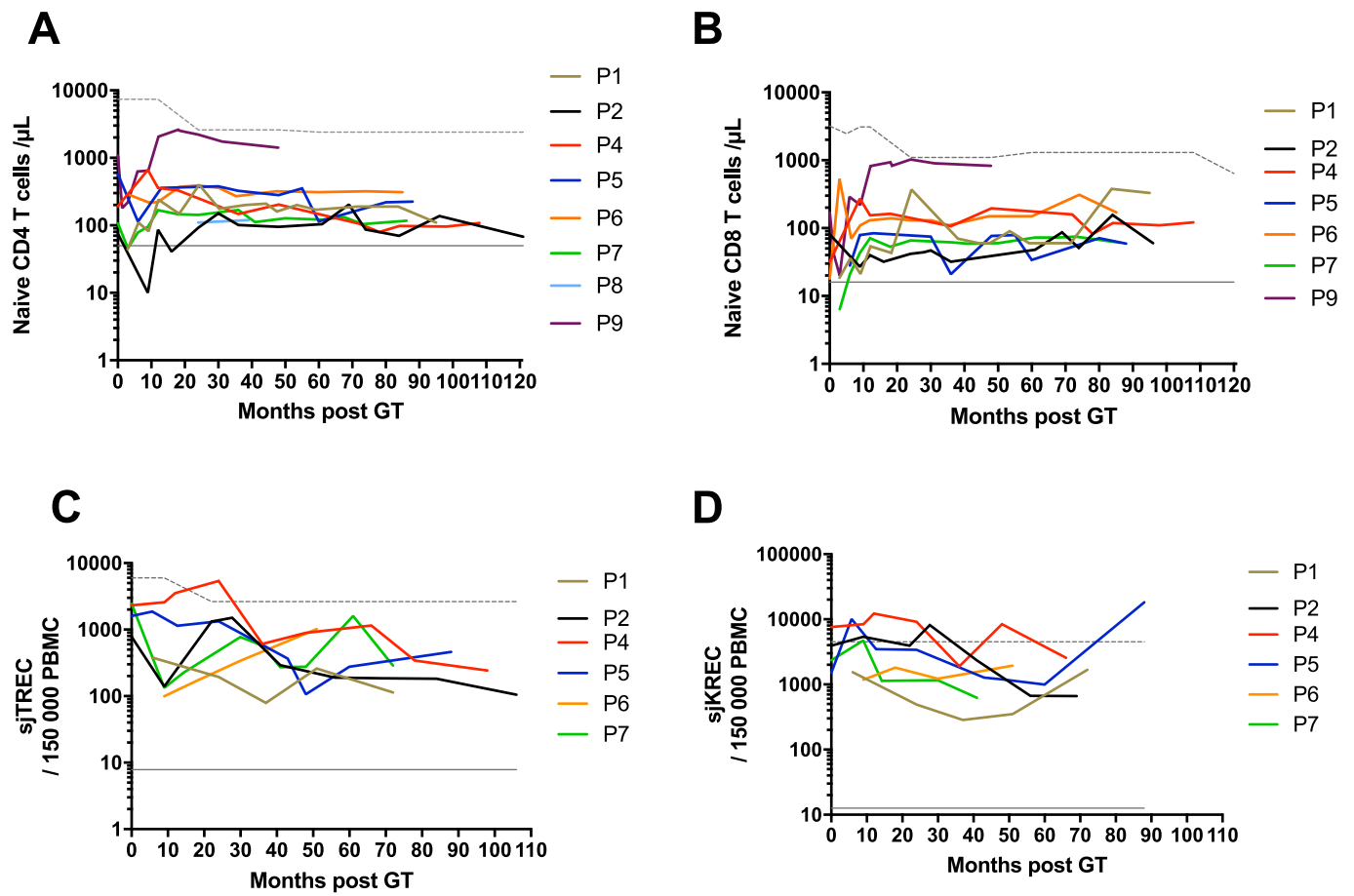
Extended Data Fig. 1 | Clinical and laboratory features of patients with WAS before and after GT. Clinical and laboratory features of patients with WAS before and after GT: light pink: no disease; pink: mild disease; light red: moderate disease; red: severe disease. Eczema was graded with the SCORAD tool²⁴. Infections and bleeding were graded in terms of recurrence and severity. Vasculitis was assessed according to the WAS severity scoring system⁴. Thrombocytopenia was defined as follows: grade 3 for a platelet count <10,000/ μ L; grade 2 between 10,000/ μ L and 20,000/ μ L; grade 1 between 20,000/ μ L and 50,000/ μ L. Grey box: not applicable. Statistical significance was determined by t test (***p < 0.001); NS: not significant.



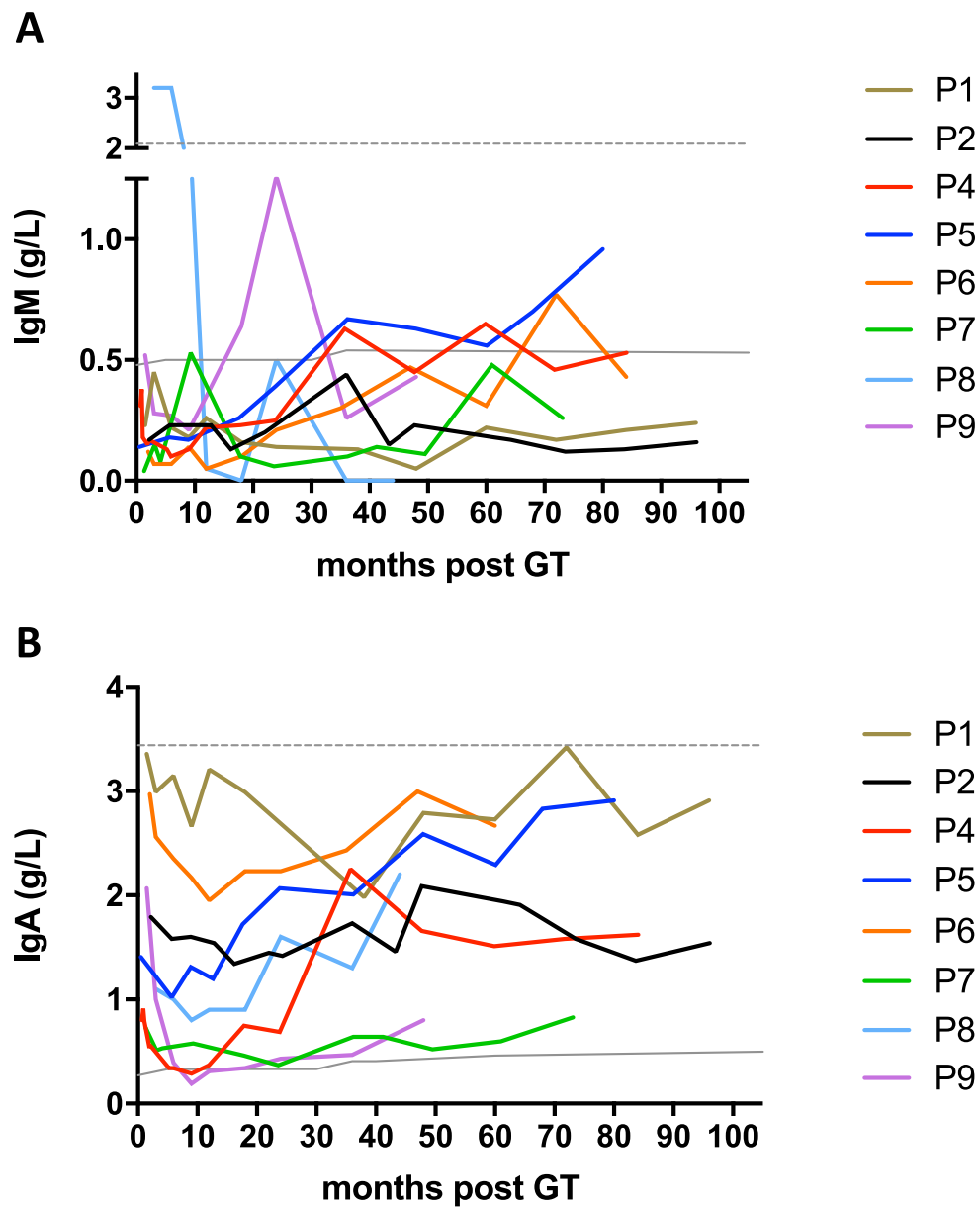
Extended Data Fig. 2 | Gene marking level. Panel A, the VCN in the bone marrow (BM, white) subpopulations versus the peripheral blood (black) subpopulations in patients P2, P4 and P5; Panel B, VCN levels in the initial CD34 + drug product versus myeloid CD15 + cells 48 months after GT. Panel C, The Spearman correlation between the level of gene marking in CD15 + 48 months after GT and the number of corrected CD34 + cells infused per kilogram, for each patient. The pvalue (p) was calculated by using two-sided Spearman’s rank correlation test, r is Spearman’s rank correlation coefficient. A regression line is represented in black, the confidence interval in grey.



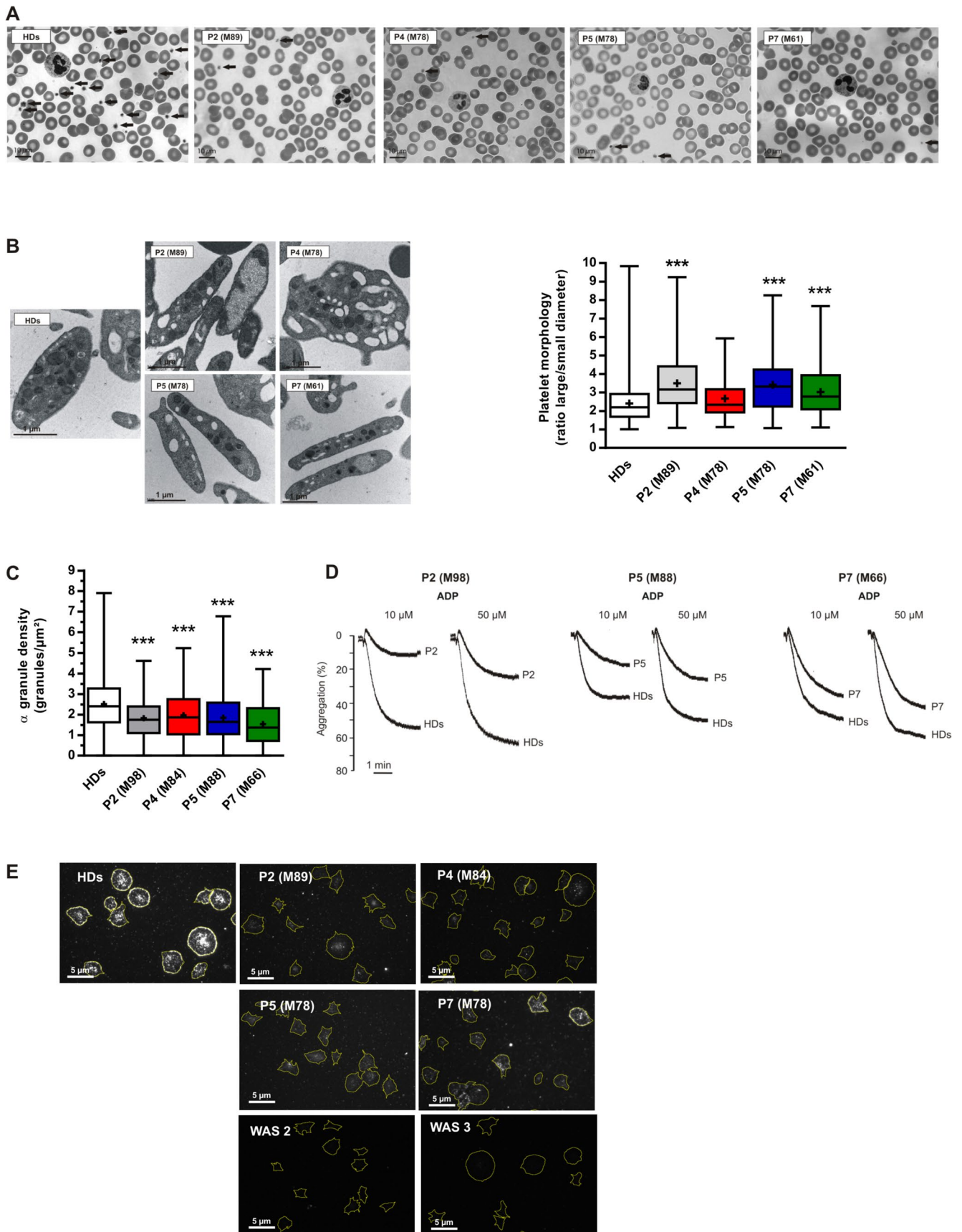
Extended Data Fig. 3 | Immunological reconstitution after GT. Immunological reconstitution after GT with age-matched reference values adjusted for each patient, CD3+ (Panel A), CD19+ (Panel B), CD56+ (Panel C) and CD15+ (Panel D). Age-matched reference values are indicated by the grey lines (mean values, dashed lines, lower and upper values, dotted lines).



Extended Data Fig. 4 | Immunological reconstitution after GT. Immunological reconstitution after GT of naive CD4+ T cells, CD4+CD45RA+CD31+ cells (Panel A), naive CD8+ T cells, CD8+CD45RA+CCR7+ cells (Panel B), Tcell receptor excision circles (sjTRECs) (Panel C) and immunoglobulin kappa-deleting recombination excision circles (sjKREC) (Panel D). Age-matched reference values are indicated by the grey lines (solid line: lower value; dashed line: upper value).

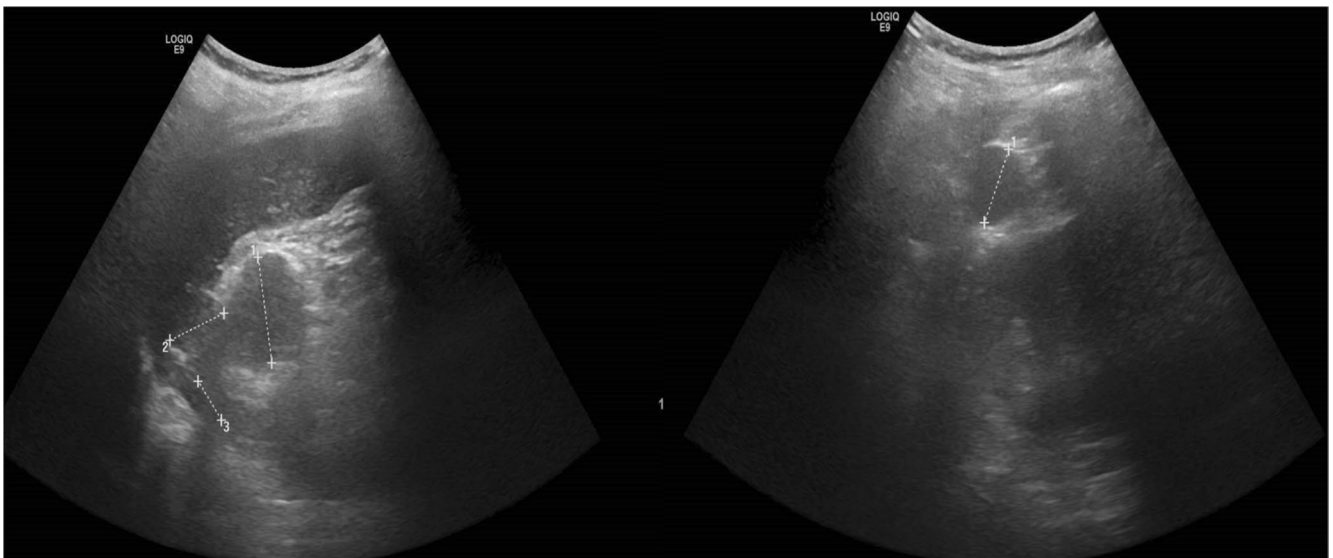


Extended Data Fig. 5 | Immunoglobulin reconstitution after GT. Immunoglobulin (Ig) reconstitution after GT. Panel A, IgM production over time; Panel B, IgA production over time. Age-matched reference values are indicated by the grey lines (solid line: lower value; dashed line: upper value).

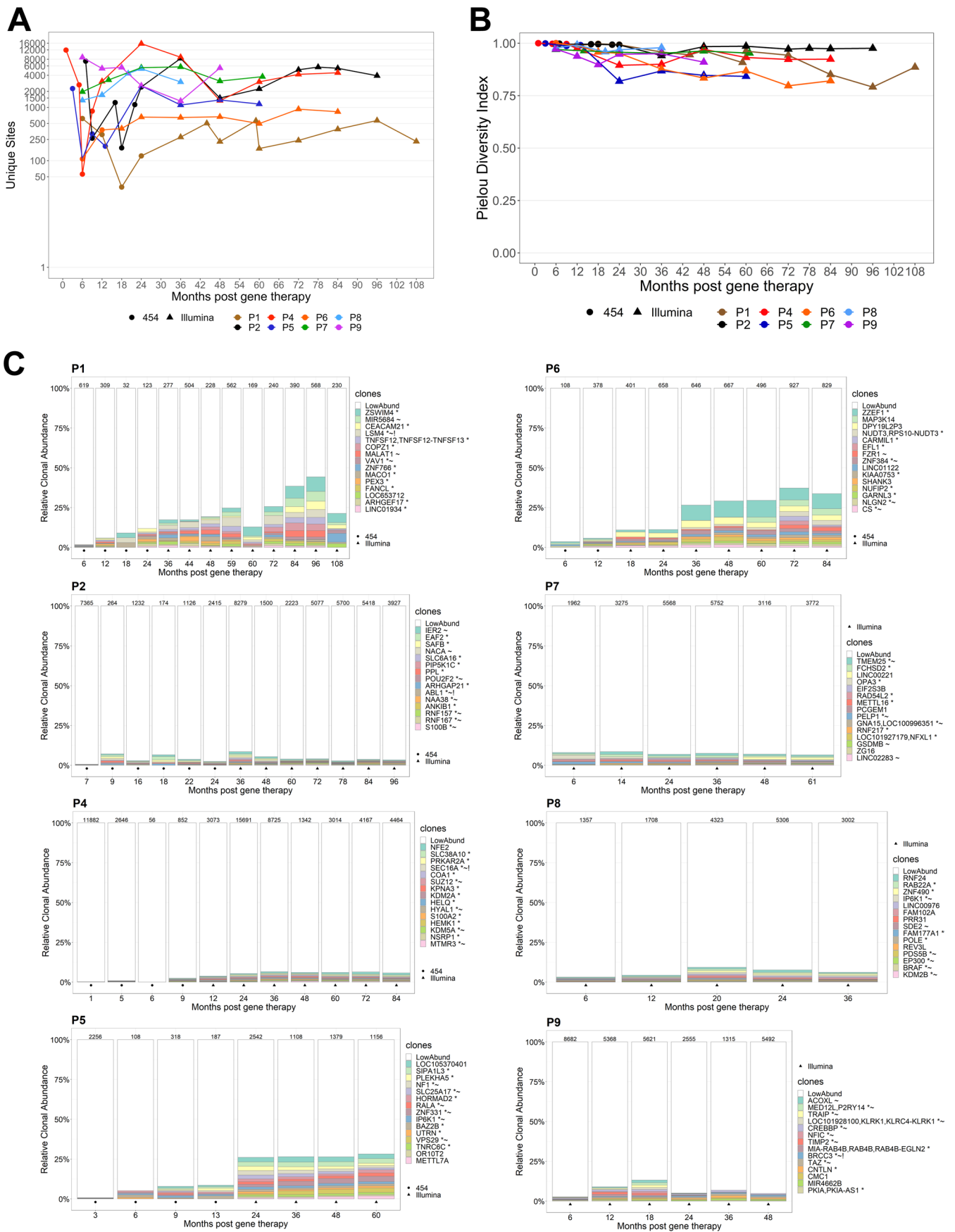


Extended Data Fig. 6 | See next page for caption.

Extended Data Fig. 6 | Platelet analyses. Panel A, Images show blood smears performed once for each GT-treated patients (P) or healthy donors (HDs) after May-Grünwald Giemsa staining. Arrows indicate the platelets. Panel B, TEM analysis of platelet ultrastructure in each patient (P). The box-and-whisker plots show the platelet shape defined as the ratio between the largest diameter and the smallest diameter derived from the TEM images performed once for each patient. Whiskers represent the upper and lower extreme values, the box correspond to the interquartile range, the center line is the median and the cross indicates the mean of 100 platelets for patients and 826 platelets for HDs. Statistical significance was determined in a one-way ANOVA with the Sidak post-test for multiple comparisons. The exact p value was $p < 0.0001$ for P2, P5, P7 and $p = 0.1484$ for P4. Panel C, the α -granule density for each patient was quantified by TEM and the results were shown in box-and-whisker plots. Whiskers represent the upper and lower extreme values, the box correspond to the interquartile range, the center line is the median and the cross indicates the mean of 100 platelets for patients and 970 for HDs. Statistical significance was determined in a one-way ANOVA with the Sidak post-test for multiple comparisons. The exact p value was $p < 0.0001$ for all P2, P5, P7 and $p = 0.0002$ for P4. Panel D, Aggregation of washed platelets induced by ADP (10 or 50 μ M) was evaluated once for P2, P5 and P7. Panel E, WASp expression was evaluated by immunofluorescence in platelets spread onto a fibrinogen matrix after activation with 20 μ M ADP. WASp was detected using a specific antibody. The outlines of spread platelets (represented by the yellow lines) were identified by detecting F-actin with fluorescently labeled phalloidin.



Extended Data Fig. 7 | Ultrasound assessment of P2. Ultrasound assessment of P2, showing three accessory spleens (measuring up to 3 cm in diameter) in the right hypochondrium.



Extended Data Fig. 8 | See next page for caption.

Extended Data Fig. 8 | Integration site (IS) analyses. Panel A, The number of unique ISs detected in PBMCs at various points (in months) after gene therapy. Most of the samples were analyzed by sonic shearing in Illumina sequencing experiments (triangle), except that the early samples were analyzed using restriction endonucleases in 454 sequencing experiments (circle). Panel B, The Pielou diversity index for the IS population in PBMCs for the different patients. Panel C, A stacked bar representation showing the relative clone size (sonic abundance) of the TOP15 integration site clones detected over time for each patient.

Reporting Summary

Nature Research wishes to improve the reproducibility of the work that we publish. This form provides structure for consistency and transparency in reporting. For further information on Nature Research policies, see our [Editorial Policies](#) and the [Editorial Policy Checklist](#).

Statistics

For all statistical analyses, confirm that the following items are present in the figure legend, table legend, main text, or Methods section.

- | | |
|-------------------------------------|--|
| n/a | Confirmed |
| <input type="checkbox"/> | <input checked="" type="checkbox"/> The exact sample size (n) for each experimental group/condition, given as a discrete number and unit of measurement |
| <input checked="" type="checkbox"/> | <input type="checkbox"/> A statement on whether measurements were taken from distinct samples or whether the same sample was measured repeatedly |
| <input type="checkbox"/> | <input checked="" type="checkbox"/> The statistical test(s) used AND whether they are one- or two-sided
<i>Only common tests should be described solely by name; describe more complex techniques in the Methods section.</i> |
| <input checked="" type="checkbox"/> | <input type="checkbox"/> A description of all covariates tested |
| <input checked="" type="checkbox"/> | <input type="checkbox"/> A description of any assumptions or corrections, such as tests of normality and adjustment for multiple comparisons |
| <input type="checkbox"/> | <input checked="" type="checkbox"/> A full description of the statistical parameters including central tendency (e.g. means) or other basic estimates (e.g. regression coefficient) AND variation (e.g. standard deviation) or associated estimates of uncertainty (e.g. confidence intervals) |
| <input type="checkbox"/> | <input checked="" type="checkbox"/> For null hypothesis testing, the test statistic (e.g. F , t , r) with confidence intervals, effect sizes, degrees of freedom and P value noted
<i>Give P values as exact values whenever suitable.</i> |
| <input checked="" type="checkbox"/> | <input type="checkbox"/> For Bayesian analysis, information on the choice of priors and Markov chain Monte Carlo settings |
| <input checked="" type="checkbox"/> | <input type="checkbox"/> For hierarchical and complex designs, identification of the appropriate level for tests and full reporting of outcomes |
| <input checked="" type="checkbox"/> | <input type="checkbox"/> Estimates of effect sizes (e.g. Cohen's d , Pearson's r), indicating how they were calculated |

Our web collection on [statistics for biologists](#) contains articles on many of the points above.

Software and code

Policy information about [availability of computer code](#)

Data collection Data were collected manually and transferred to Altizem society for data management through Clintrial software

Data analysis Figures were prepared with Software R (R core team (2019). R version 4.0.4. R foundation for Statistical Computing, Vienna, Austria. URL <https://www.R-project.org/>). Shannon diversity index were calculated using the vegan package. Circos plots, showing the various V-gene and J-gene combinations, were designed using the circlize package. Flow cytometry data were analyzed using FlowJo software (TreeStar) (FlowJo v10.5.3). WASp expression was quantified using ImageJ software (ImageJ 1.X). WASP expression western blot was analyzed via Gene Tools software (version 4.03.05.0; Syngene, Cambridge, UK). Statistical analyses were performed using the INSPIRED pipeline (<https://github.com/BushmanLab/INSPIRED>). All the sequence data used in the present study are available in the NCBI Sequence Research Archive (SRA, reference: SRP050221 and PRJNA685802).

For manuscripts utilizing custom algorithms or software that are central to the research but not yet described in published literature, software must be made available to editors and reviewers. We strongly encourage code deposition in a community repository (e.g. GitHub). See the Nature Research [guidelines for submitting code & software](#) for further information.

Data

Policy information about [availability of data](#)

All manuscripts must include a [data availability statement](#). This statement should provide the following information, where applicable:

- Accession codes, unique identifiers, or web links for publicly available datasets
- A list of figures that have associated raw data
- A description of any restrictions on data availability

Data that support the findings in this study are available from the authors upon agreement of the sponsor (Genethon). Restrictions may apply to the availability of these data before the end of the study as they are part of clinical trials, subject to patient confidentiality and are not public. Integration sites sequence data used in

the present study are available in the NCBI Sequence Research Archive (SRA, reference: SRP050221 and PRJNA685802). TCR NGS sequence data and RCL analyses are available upon request.

Inquiries for access to the study clinical data can be submitted to Dr. S. Abbas, Genethon Clinical Development Department (1bis, Rue de l'Internationale, 91000 EVRY - France, Phone: +33 (0)1 69 47 28 28, Fax: +33 (0)1 69 47 19 46) and inquiries will be addressed within 30 working days.

Field-specific reporting

Please select the one below that is the best fit for your research. If you are not sure, read the appropriate sections before making your selection.

Life sciences Behavioural & social sciences Ecological, evolutionary & environmental sciences

For a reference copy of the document with all sections, see [nature.com/documents/nr-reporting-summary-flat.pdf](https://www.nature.com/documents/nr-reporting-summary-flat.pdf)

Life sciences study design

All studies must disclose on these points even when the disclosure is negative.

Sample size	This is a long term follow-up study that includes the patients from the two previous studies NCT01347346- and NCT01347242.
Data exclusions	None
Replication	In this clinical study, each sample analyzed is a unique sample.
Randomization	This is a longitudinal follow-up study that includes the patients from two previous non-randomized phase I/II studies NCT01347346- and NCT01347242.
Blinding	Blinding is not applicable for autologous gene therapy.

Reporting for specific materials, systems and methods

We require information from authors about some types of materials, experimental systems and methods used in many studies. Here, indicate whether each material, system or method listed is relevant to your study. If you are not sure if a list item applies to your research, read the appropriate section before selecting a response.

Materials & experimental systems

n/a	Involved in the study
<input type="checkbox"/>	<input checked="" type="checkbox"/> Antibodies
<input type="checkbox"/>	<input checked="" type="checkbox"/> Eukaryotic cell lines
<input checked="" type="checkbox"/>	<input type="checkbox"/> Palaeontology and archaeology
<input checked="" type="checkbox"/>	<input type="checkbox"/> Animals and other organisms
<input type="checkbox"/>	<input checked="" type="checkbox"/> Human research participants
<input type="checkbox"/>	<input checked="" type="checkbox"/> Clinical data
<input checked="" type="checkbox"/>	<input type="checkbox"/> Dual use research of concern

Methods

n/a	Involved in the study
<input checked="" type="checkbox"/>	<input type="checkbox"/> ChIP-seq
<input checked="" type="checkbox"/>	<input type="checkbox"/> Flow cytometry
<input checked="" type="checkbox"/>	<input type="checkbox"/> MRI-based neuroimaging

Antibodies

Antibodies used

anti-CD3 monoclonal antibody (mAb) (10 µg/ml OKT3, eBioscience); . Unlabeled a24 mAb (Biolegend) that binds to LFA-1 in its high-affinity conformation at a concentration of 2.5 µg/ml; with phalloidin-AF488 (Invitrogen), and anti-WASp rabbit mAbs (Abcam ab75830). The anti-LFA-1 and WASp Abs were then revealed with anti-mouse AF647-coupled and anti-rabbit AF564-coupled secondary Abs (Invitrogen), respectively. BD Accuri C6 flow cytometer (BD Biosciences). mouse anti-WASp primary antibody (1 µg/mL, clone B-9; Santa Cruz; Heidelberg, Germany) or mouse anti-CD41 (0.2 µg/mL, clone SZ22, used as loading control for normalization; Beckman Coulter). goat anti-mouse IgG Alexa Fluor 555 conjugate (4 µg/mL; Invitrogen); cytoskeletal F-actin with Alexa Fluor 488-phalloidin (0.3 µM; Invitrogen). The patients' antiplatelet antibodies were detected using the "monoclonal antibody-specific immobilization of platelet antigen" technique, according to the manufacturer's instructions (apDia, Turnhout, Belgium).

Validation

Each antibody used had a validated technical data sheet as per manufacturer's website showing positive staining.

Eukaryotic cell lines

Policy information about [cell lines](#)

Cell line source(s)

P815 (RRID:CVCL_2154)

Authentication	Cells line was not authenticated
Mycoplasma contamination	Mycoplasma free
Commonly misidentified lines (See ICLAC register)	The cell line used is not listed in the ICLAC database

Human research participants

Policy information about [studies involving human research participants](#)

Population characteristics	All the information are detailed in the dedicated clinical trial web page: Clinical trials.gov : NCT01347346, Clinical trials.gov : NCT01347242 ClinicalTrials.gov Identifier: NCT02333760
Recruitment	Participants recruited to the study are WAS patients enrolled and treated in the phase I/II studies conducted in France and United Kingdom (NCT01347346- and NCT01347242) and with signed informed consent.
Ethics oversight	The protocols conducted in France and in the UK were approved by the respective national regulatory authorities : the UK MHRA (Medicines and Healthcare Products Regulatory Agency) with advice from the Gene Therapy Advisory Committee (GTAC) and local R&D committee ; in France by the ANSM (Agence Nationale de Sécurité du Médicament et des Produits de Santé) with approval from a CPP Committee (Comité pour la Protection des Personnes).

Note that full information on the approval of the study protocol must also be provided in the manuscript.

Clinical data

Policy information about [clinical studies](#)

All manuscripts should comply with the ICMJE [guidelines for publication of clinical research](#) and a completed [CONSORT checklist](#) must be included with all submissions.

Clinical trial registration	Clinical trials.gov : NCT01347346; Clinical trials.gov : NCT01347242; ClinicalTrials.gov : NCT02333760
Study protocol	Data that support the findings is in the study protocol and in the protocol synopsis which is available and is public on https://clinicaltrials.gov/ under NCT number 02333760 , the study protocol is available from the authors upon agreement of the sponsor (Genethon). Restriction may apply to study protocol publication as supplement material due to the confidentiality of data and are not public
Data collection	Data were collected on the study sites (Hospital Necker, Paris, France), GOSH, London and UCLH, London) and monitored by Genethon from Period of 2014 to 2018, and then after "CRA plateforme" ,clinical trial management provider selected by GENETHON , collect data and monitored the trial from 2018 to date . Pharmacovigilance was conducted by AXPharma, Paris, under GENETHON control and validation.
Outcomes	Primary outcomes of the long term study were to establish clinical and biological safety, efficacy and tolerability by evaluating the incidence and type of serious adverse events, the clinical status and biological parameters including lentiviral genomic integration sites in different cells sub-populations from 3 years to 15 years post GT. Secondary outcomes included monitoring the need for additional treatments and T cell repertoire diversity. See Clinical trials.gov : NCT01347346; Clinical trials.gov : NCT01347242; ClinicalTrials.gov : NCT02333760